Albert-Ludwigs-Universität Freiburg

Master Thesis

Assessing the temporal and spatial runoff generation processes in a headwater catchment

Author:
Sven C.M. DECKER

Supervisor:
Prof. Dr. Markus WEILER

Chair of Hydrology
Faculty of Environment and Natural Resources

27^{th} November of 2015

Albert-Ludwigs-Universität Freiburg

Master Thesis

Assessing the temporal and spatial runoff generation processes in a headwater catchment

Author:
Sven C.M. DECKER

Supervisor:
Prof. Dr. Markus WEILER
Co-Supervisor:
Prof. Dr. Jan SEIBERT

A thesis submitted in fulfillment of the requirements for the degree of Master of Science

in the

Chair of Hydrology
Faculty of Environment and Natural Resources

27^{th} November of 2015

Abstract

Flow path dynamics, particularly those of subsurface flows, are crucial for the understanding of temporal and spatial runoff generation processes in steep forested catchments with humid climate. In a headwater catchment near Freiburg previous research was pursued using environmental and fluorescent tracing. On three adjacent slopes which differ only in vegetation cover uranine was injected in 2 m soil depth. Tracer flow and thereby subsurface flow paths were aimed to be detected by monitoring several sites downslope. Additionally, hydrochemistry and isotopes were measured with high resolution (1.5 - 24 h) at two sites in the creek and at one perennial hillslope source. This thesis investigates double-peak events (two discharge peaks by one rainfall) - a phenomena known to occur in the catchment.

Due to a long summer drought almost no subsurface flow occurred and no tracer could be detected at the measurement sites. Instead, interesting characteristics of the hillslope source were observed leading to the idea of a fractured aquifer with a specific drainage pattern due to the underlying periglacial drift cover layers. Hydrochemical data also showed a kind of hysteresis effect on the catchment outlet indicating a different response of the catchment to seasonal preconditions. Here, further investigations are necessary. Comparing the discharge in the creek, one hypothesis for the origin of the double-peak events could probably be discarded: the double-peaks do not seem to origin from geologic differences in the catchment. Certainly just one double-peak event could be observed during the study period.

Keywords: hillslope hydrology, subsurface flow paths, uranine, environmental tracer, double-peak events, runoff generation, headwater catchment.

Zusammenfassung

Zur Bestimmung von Abflussbildungsprozessen in steilen, bewaldeten Kopfeinzugsgebieten in humiden Klimaten ist es entscheidend Kenntnis über die verschiedenen Fließwege des Wassers über und durch die Hänge zu haben. Die vorliegende Arbeit erweitert die bisherige Forschung in einem kleinen Einzugsgebiet nahe Freiburg um den Einsatz von Umwelt- und Fluoreszenztracern. Darüber hinaus wurde im Einzugsgebiet zusätzlich zum Einzugsgebietsauslass an einer geoloischen Grenze ein Wehr installiert und eine ganzjähig wasserführende Hangquelle gefasst. An drei benachbarten Hängen wurde Uranin in 2 m Bodentiefe eingespeist. Die Hänge unterscheiden sich lediglich in der Vegetationsbedeckung. Über einen Nachweis des Tracers entweder im Bach oder an den Gräben, sollte auf unterschiedliche Fließwege geschlossen werden. Zusätzlich wurde an den Wehren und der Hangquelle kontinuielich (in Intervallen von 1.5 - 24 h) die Hydrochemie und das Isotopenverhältnis gemessen.

Aufgrund eines heißen und trockenen Sommers kam es zu keinem Abfluss in bzw. an den Hängen. Dadurch wurde auch kein Tracer transportiert. Stattdessen zeigen die hydrochemischen Daten einige interessante Dinge: Im unteren Bereich des Baches scheint es einen Hysterese Effekt zu geben. Abhängig von der Jahrezeit ist die hydrochemische Zusammensetzung des Wasser bei gleichem Abfluss unterschiedlich. Kombiniert mit dem (geringen) Tracernachweis und den Isotopendaten der Hangquelle ergibt sich das Konzept eines Grundwasserspeichers, der die Quelle speist. Die Hydrochemischen Daten lassen zudem die Vermutung aufkommen, dass der Aquifer entsprechend der Schichtung der zugrundeliegenden periglazialen Hangschuttlagen verschiedene Speicher hat.

Stichworte: Hanghydrologie, Uranin, Umwelttracer, Double-peak events, Abflussbildungsprozesse, Kopfeinzugsgebiet.

The trick is to combine your waking rational abilities
with the infinite possibilities of your dreams.
Because, if you can do that, you can do anything.

- Waking Life, 2001 -

Acknowledgements

I am very grateful for all supporting me during my studies and in particular to fulfill this thesis.

Especially I would like to thank...

... Prof. Dr. Markus Weiler for supervising this thesis.

... Prof. Dr. Jan Seibert for assuming the co-supervision.

... Matthias Ritter for advice at any time and assistance during fieldwork.

... Emil Blattmann and Britta Kattenstroth for their assistance setting up the measurement setup.

... Barbara Herbstritt, Petra Küfner and Harald Unrein for supporting me in the laboratory.

... my fellow students for fruitful discussions and joyful distraction.

... my family for their tenderly and firm encouragement.

Thank you all!

Declaration of authorship

I, Sven DECKER, declare that this thesis titled, 'Assessing the temporal and spatial runoff generation processes in a headwater catchment' and the work presented in it are my own. I confirm that:

- This work was done wholly or mainly while in candidature for a research degree at this University.
- Where any part of this thesis has previously been submitted for a degree or any other qualification at this University or any other institution, this has been clearly stated.
- Where I have consulted the published work of others, this is always clearly attributed.
- Where I have quoted from the work of others, the source is always given. With the exception of such quotations, this thesis is entirely my own work.
- I have acknowledged all main sources of help.
- Where the thesis is based on work done by myself jointly with others, I have made clear exactly what was done by others and what I have contributed myself.

Place, Date

Signature

Contents

List of Figures

List of Tables

1 Introduction

Solid understanding of hydrological dynamics and processes as well as knowledge about the interactions between soil, vegetation and atmosphere at the hillslope scale are necessary for predictions about ungauged hillslopes and catchments dominated by subsurface flow (Bachmair and Weiler, 2012). Subsurface flow (SSF) is the main source of storm discharge in common humid, soil-covered, vegetated headwater regions (Anderson et al., 1997). It is necessary to gain solid knowledge about SSF to improve e.g. flood forecasting, risk management of hillslope instabilities or pollutant transport. SSF domninates the hydrological regime (transport of solutes and nutrients), and can affect hillslope stability, especially in steep forested watersheds in humid climates (Anderson et al., 2009). Although SSF and related processes like preferential flow are important factors, the mechanisms of SSF are largely unknown (Anderson et al., 2009). A common problem occuring on hillslope hydrology is that the uniqueness of each study site can dominate general processes (Uchida et al., 2006; Weiler and McDonnell, 2004).

Bachmair (2012) states that "a prerequisite for deriving generalizable process understanding about hillslope hydrological dynamics and their governing factors is a) monitoring largerscale hillslopes over longer time to capture the high spatiotemporal variability of processes, and b) intercomparing hillslopes differing in certain characteristics while others remain constant (e.g. bedrock, soil, topography, vegetation cover) to systematically control governing factors".

This thesis will pursue the work done in a steep headwater catchment on SSF and extend it to environmental and fluorescent tracer studies. The aim is to gain information about SSF flowpaths through the hillslopes and to investigate the origin of occurring double-peak events.

1.1 State of the art

Based on Bachmair and Weiler (2011) the general idea of hillslope hydrological processes is described here, pointing out important and recent concepts of hillslope hydrology. The basic concept is shown in figure 1. The figure shows relevant flow paths that contribute to runoff generation. These are:

- Hortonian or saturation overland flow (HOF or SOF)
- Biomat or near surface flow

- Subsurface flow (SSF)
- Pipe flow
- Deep percolation (DP)

HOF, or infiltration excess overland flow, is a lateral flow along the surface and occurs when rainfall intensity exceeds the infiltration capacity of the soil. It rarely occurs on forested catchments except on silk roads, trails or as return flow of saturated or low permeable areas (Sidle et al., 2007). Factors favouring HOF are surface sealing, crust building soil compaction, an abrupt increase of bulk intensity, topsoil hydrophobicity and low macroporosity (Doerr et al., 2000; Scherrer and Naef, 2003; Schmocker-Fackel, 2004; Weiler and Naef, 2003). It is initiated when the storage capacity of the soil is reached and the soil is saturated. SOF depends on antecedent wetness and preferential flow paths. Surface runoff flow paths are influenced by surface roughness like stones, vegetation or microrelief, reinfiltration, and run-on processes (Bracken and Croke, 2007; Corradini et al., 1998).

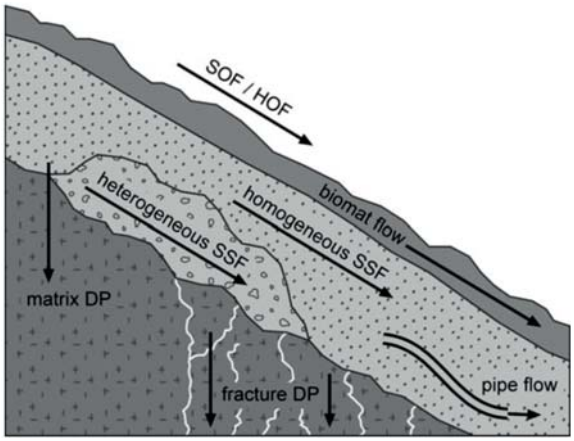

Figure 1: Conceptual hillslope model (Bachmair and Weiler, 2011).

It is important to distinguish biomat flow and HOF. Often it is mistakenly assumed to be the same but infact near surface flow or biomat flow is runoff through the forest litter layer. In the literature such flowpaths are also known as 'organic layer interflow', 'pseudo-overland flow' and 'thatched roof' effect (McDonnell et al., 1991; Sidle et al., 2007; Weiler and McDonnell, 2004). Recent research by Gerke et al. (2015) stated that the biomat layer can be devided into two sub-layers with different structures.

SSF, also known as interflow, throughflow, lateral flow, or shallow groundwater flow, is the fast lateral movement of water through the soil or permeable bedrock above a layer of reduced permeability (Dunne, 1978; Weiler et al., 2006). It occurs as lateral preferential flow due to high spatial variability of controlling factors. SSF is indicated by a limited water table response by increasing discharge if a preferential network exists and is already activated (Anderson et al., 2009). To initiate SSF, partial saturation of soil in areas of low permeability (bedrock or soil layers) is necessary. Then SSF can take place through layers of high permeability or soil pipes. High permeable layers are characterized e.g. by high texture. They can be found on landslide debris, periglacial solifluction deposits, or unconsolidated moraine material (Weiler et al., 2006). SSF is the factor dominating runoff generation in steep, deep weathered catchments with humid climate (Wagener et al., 2007).

Soil pipes can be decayed roots or animal burrows and are lateral voids evolving also from subsurface hydraulic erosion. They can be found along the whole soil profile whether disconnected or connected to networks (Uchida et al., 2001; Weiler et al., 2006). The exact mechanisms of pipe flow initiation, inter-connection and exchange processes with surrounding soil still remain mostly unkown (Bachmair and Weiler, 2011). Uchida et al. (2001) points out that pipe flow can increase slope stability by increasing the rate of slope drainage capacity. However, once the incoming water exceeds the drainage capacity of the pipe flow network, the pipes fill up with water and pore water pressure increases in the surrounding matrix, destabilizing the slope.

Groundwater recharge or DP occurs when water moves vertically into the bedrock. It is characterized by old or pre-event water, whereas HOF or SOF almost only consists of event or new water. SSF is a mixture of those water types showing a high variability in ratios due to high variability in flow path characteristics.

Especially SSF and DP were underestimated in early studies as it was assumed that underlaying bedrock is impermeable. Nowadays it is known that not only infiltration into the bedrock but also exfiltration from the bedrock are significant.

Looking at the response parameters of a hillslope (response time, water transit time and event to pre-event water ratio), they differ by the pathway taken by the incoming precipitation. DP generally has long transit times and mainly pre-event water whereas HOF/SOF have short transit times and a high amount of event water.

All the flow processes listed above are controlled by different environmental factors. Those can be divided into static and dynamic ones. Static factors are parent material, surface and bedrock topography, and exposure. These are stable at least for shorter time scales in geological standards. Precipitation characteristics, soil moisture, and vegetation are defined as dynamic factors. They underlie seasonal effects and current weather conditions and vary over time (Bachmair and Weiler, 2011).

Here both groups will be presented in more detail. Beginning with the dynamic factors the input to hillslopes is essential. Input is the precipitation. The system's reaction to it depends on the amount, intensity, frequency, and state (i.e. snow or rain) of precipitation. If the input is as snow, the characteristics of snow pack and the timing of snow melt should be taken into consideration. Between precipitation input and hillslope response there seems to be a strong non-linearity. Some studies found that a precipitation threshold had to be exceeded before a significant hillslope outflow was triggered (Graham and McDonnell, 2010; McGuire and McDonnell, 2010; Tromp-Van Meerveld and McDonnell, 2006a). Tromp-Van Meerveld and McDonnell (2006a) analysed a 147-storm data set from Panola hillslope and determined a precipitation threshold of 55 mm before the preferential flow network is activated. They also discovered a linear relationship between total pipe flow and subsurface storm flow. McGuire and McDonnell (2010) state a 20 mm threshold with a linear discharge response when the threshold is exceeded. Graham and McDonnell (2010) show that the threshold behaviour depends on both environmental and geological factors.

Another important dynamic factor underlying at least seasonal variation is the vegetation cover of the hillslope. Typical characteristics of forested catchments are higher evapotranspiration, lower runoff, delayed peak flow and a longer hydrograph recession time (Jost et al., 2005; Schume et al., 2004). Precipitation is separated by vegetation both above and below the ground (and on the ground).
Above-ground separation of precipitation by vegetation can be distinguished into interception, stemflow and throughfall (Crockford and Richardson, 2000). Interception of precipitation on forest canopies results in temporal storage and intensity smoothing and additionally higher evaporation. Stemflow leads to spatial variable soil moisture patterns (Johnson and Lehmann, 2006; Levia et al., 2010).
On and below the ground water is separated by near-surface vegetation, organic litter layer and roots. The organic litter layer can be a barrier for infiltration leading to surface runoff, or vice versa. There are differences in the reaction of this layer depending on the leaf type. Broad-leaf litter layer intercepts more water than a needle-leaf litter layer and water moves laterally whereas in a needle-leaf litter layer water moves vertically (Sato et al., 2004). Schume et al. (2004) observed that spruce needle-leaf litter layer might be hydrophobic and prevent vertical infiltration. A similar effect occurs on dry, fur-like root layers on grassland topsoil, alpine mats, and burned areas (Doerr et al., 2000; Scherrer et al., 2006). Moreover, seasonal variations in vegetation affect the characteristics of the litter layer, separation of precipitation and runoff generation (Bachmair and Weiler, 2011). Below ground, vegetation affects the way the water takes downslope by contributing to the development of preferential flow paths along roots (Buttle, 2002). Recent research brought different root systems into focus: Nordmann et al. (2009) showed significant differences with regard to how root systems can affect SSF. One can distinguish between taproot, heart-shaped, and sinker root systems. Deep-rooting trees lead to higher retention rates than shallow rooting ones.

Looking at the static factors, it is quite obvious that topography is an important factor driving not only the hydrology but also affecting soil properties, vegetation pattern and microclimate. Interesting parameters when looking at topography are slope gradient, hillslope geometry, exposition and micro-topography. With respect to topography, hillslopes can be characterized by the profile curvature (convex, planar and concave) and the planform curvature (divergent, parallel, convergent). These parameters and characterization affect runoff generation, flow behaviour and saturation along hillslopes (Bachmair and Weiler, 2011). Recent research has set a mathematical formulation (hillslope storage Boussinesq equation) for homogenous SSF on complex hillslopes showing that convergent hillslopes drain more slowly than divergent ones (Troch et al., 2003). Not just the surface topography but also the bedrock topography influences the runoff generation. Tromp-Van Meerveld and McDonnell (2006b) described the 'fill-and-spill' concept as explanation for the threshold behaviour of the discharge to periciptation. Bedrock depressions have to be filled up before water spills over the edge and generates a flow path network contributing to runoff. Graham and McDonnell (2010) described the same concept and Spence and Woo (2003) described a similar concept for arctic

valley groundwater. Bachmair and Weiler (2011) described a similar concept, too, but based on hydrological active areas which need to be connected to trigger a significant reaction (the concept of 'connect-and-react').

Another static parameter is the type of soil controlling that part of the incoming precipitation that infiltrates into the ground and of course also the infiltration itself. Controlling factors are the soil type, thickness, drainable porosity, pipes, macropores, and moisture content. A certain soil type results in a certain hydrological reaction. Soil thickness and drainable porosity give information about short-time storage capacity and SSF possibilities. The network of soil pipes and macropores seems to be part of most hillslopes and seems to influence hillslope hydrology to a large extend. But the evolution and maintenance of these networks is still not totally understood. Pipe networks seem to be an interaction of mechanical processes, soil, topography, climate and the contributing area. Mechanical processes can be driven by burrowing animals, roots or subsurface erosion (Tsuboyama et al., 1994).

At last the impact of soil moisture must be mentioned. Not only soil moisture itself is important but also whether moist soil patterns are connected or not. "Generally, the wetter the system, the faster and more intense the hydrologic response will be." (Bachmair and Weiler, 2011). Soil moisture thus underlies not only a high spatial variability as mentioned above but also a high temporal one. It is dependent on the season and the current weather conditions. This includes dependency on the state of vegetation as transpiration varies within the year and day. McNamara et al. (2005) defined five soil moisture states throughout the year for a semi-arid, snowmelt-driven catchment: 1. a summer dry period, 2. a transitional fall wetting period, 3. a winter wet, low-flux period, 4. a spring wet, high-flux period, and 5. a transitional late-spring drying period.

Looking at the geological setting of a catchment, the bedrock topography and the bedrock permeability are interesting parameters affecting hydrological hillslope response. Bedrock permeability controls the amount of water percolating vertically or draining laterally. Former studies often assumed impermeable bedrock. But bedrock topography and permeability affect runoff generation processes and SSF. E.g. Tromp-van Meerveld et al. (2007) found that at least 20 % of precipitation infiltrates into granite bedrock during large rainstorms but also that lateral subsurface flow over the bedrock surface occurs. The study was conducted in a mainly forested catchment in humid climate (Panola hillslope). Gabrielli et al. (2012) used a drilling system to investigate bedrock groundwater dynamics to hillslope runoff and described a reaction of the bedrock groundwater level during high storm events. Tromp-van Meerveld and Weiler (2008) investigated the model complexity to simulate hillslope outflow and internal hillslope dynamics. They included bedrock permeability, variable soil depth and preferential flow. When bedrock is assumed to be impermeable SSF is overpredicted in models, hillslopes stay too wet between events and recessions are too slow resulting in continuous baseflow from the slopes.

Many dye tracer applications were conducted in hillslope hydrology to find distinct preferential flow pathways (Anderson et al., 2009; Blume et al., 2008; Lange et al., 2008). Natural tracers like environmental isotopes and geochemical composition are widely used, too (McGuire et al., 2007; Uhlenbrook et al., 2008; Vogel et al., 2010). Popular for the visualisation of preferential flow paths is dye tracing and excavation of soil profiles at the plot scale (Blume et al., 2008; Weiler and Naef, 2003). To describe the complexity of the so observed preferential flow path networks Weiler and McDonnell (2007) set up a new processed-based model. Wienhöfer et al. (2009) applied fluorescent tracer to hillslopes and investigated SSF. The tracer was injected on the slope surface under quasi-steady-state conditions. Recovery rates for uranine were very low. Flury (2003) reviews that uranine is a suitable and widely used tracer for groundwater and vadose zone hydrology.

1.2 Previous studies in the study site Au

Investigations by Bachmair show that there are significant differences between the grassland hillslope and both of the forested hillslopes (coniferous and misxed forest) regarding to subsurface flow. The grassland slope seems to react less. During summer events, with dry pre-conditions, saturation zones can be found everywhere on the hillslope but with a high spatial variability. The slopes react quite fast. During the rest of the year under wet conditions the lower part of the slopes are saturated homogeneously and react more slowly. This indicates that lateral preferential flow path networks develop under dry summer conditions. These hillslope dynamics are well reflected in catchment runoff but during some events a second discharge peak occurred without any further precipitation input. There might be additional processes in progress (Bachmair et al., 2012).

Via a partial correlation analysis and a random forest approach, Bachmair and Weiler (2012) point out that (1) a complex interplay of hillslope characteristics is driving SSF, (2) soil properties and topography show highest single explanatory power, (3) vegetation characteristics unexpectedly play a minor role and (4) the examined hillslope characteristics do not explain SSF variability sufficiently. This indicates that additional drivers like bedrock topography or preferential flow path networks influence SSF variability (Bachmair and Weiler, 2012).

Examining the interaction of runoff generation processes on the plot, hillslope and catchment scale with a cross correlation leads to the assumption that hillslope processes strongly drive catchment runoff regarding the linkage between hillslope processes (SOF/HOF and SSF) and streamflow (Bachmair and Weiler, 2014).

Ritter (2013) demonstrates the existence of deep flow paths by using sodium chloride as a tracer. Using the hydrological model HillVi Ritter finds good model fit for trench flow but no sufficient fits for the water table in the wells and the tracer transport. It is concluded that the model structure is inappropriate. Ritter also finds that the processes he investigated are independent from vegetation.

Falasca (2014) investigated groundwater - surface water interactions by temperature differences. It was found that topography cannot explain differences in inflow along the stream.

By unpublished raw data by Astrid Denk (University of Tübingen, 2014) it can be assumed that bedrock is very shallow in the lower part of the mixed forest hillslope. Recent geologic investigations by Wagner (2014) showed an upcoming rock at the mixed forest hillslope. Additionally, permanent groundwater aquifer were found at all three hillslopes slopes. Still further investigations are necessary to gain knowledge about bedrock characteristics. Wagner (2014) suggests core investigations.

2 Hypotheses

As previous investigations have assumed different pathways or yet unknown processes to cause the mentioned double-peak events (Bachmair et al., 2012) in a steep headwater catchment, this thesis applies fluorescent and environmental tracer experiments in this catchment to investigate spatial and temporal variability of runoff generation processes. The aim of this thesis is to gain knowledge about the origin of the double-peak events and runoff generation processes in general for a steep, forested headwater catchment near Freiburg. The field study was designed and adapted based on Ritter (2013). In this thesis, tracer injection in the slopes is conducted as in Ritter (2013). Additionally, measurements of the hydrochemistry and intense discharge measurements were performed. The setup is enlarged by another weir, tapping of a spring and some instruments allowing continuous or at least timed tracer measurements at different sites. This allows to investigate the assumption of different flowpaths as described above.

To supplement the results of former research in this study site, this thesis aims to find more information about different flowpaths of event water through the hillslopes. This should ideally help to understand the origin of double-peak events under spring and summer conditions. Fluorescent tracer experiments, hydrochemistry and isotope measurements, discharge measurements as well as electric conductivity, water temperature, and precipitation are monitored to gain information of the hillslope behaviour and reaction to storm events under draining conditions due to summer conditions. This implies quite dry pre-conditions of the hillslope. The study does not cover the wet and more saturated conditions in autumn and winter.

With regard to the observed double-peak events four hypotheses will be tested in this thesis:

1. The first peak originates from HOF/SOF or fast and flat SSF. The second peak is slow and flat SSF.
   In this case there would be no peak in tracer concentration in the trenches and the stream for the first peak as tracer is injected in about 2 m depth. The second peak would cause a tracer concentration peak in the trench but probably not in the creek as the uranine might get photolytic degraded. Looking at the discharge, the first peak would cause a fast peak in the creek and maybe a small peak in the trench. The second peak causes a peak in both the trench and the creek shifted time-wise.

2. The first peak is flat and fast SSF. The second peak originates from deep and

slow SSF.
In this case the first peak is similar to the second peak of the first scenario: uranine peak in trench and in both the creek and the trench a time-wise shifted peak of discharge. The second peak of this scenario will flow underneath the trench and so is only detectable in the creek.

3. The first peak is a reaction of the lower catchment area, the second a reaction of the upper catchment part - or vice versa.
Based on the geology of the catchment (see figure 2) a second weir is installed dividing the catchment into an upper and lower part (see figure 3). By comparing both weirs different reactions might be detected. If so, e.g. the peaks should be shifted time-wise and the outlet P should show two peaks whereas the upper weir shows only one.

4. Of course it might be completely different or a mixture of the hypotheses mentioned above. Also it cannot be predicted if these events occur in summer time.

3 Site description

The study site is located in Southwest Germany, 4.11 km South of Freiburg. The catchment outlet is located at 47.9570° N, 7.8378° E. It has the size of 0.21 km^2. The elevation ranges from 340 - 585 m a.s.l.. The catchment is v-shaped and has been ascribed the order of zero (Bachmair and Weiler, 2012). Three adjacent hillslopes have been monitored since 2010 (Bachmair, 2012). The slopes are assumed to be similar in topography, geology and soil properties but different with regard to vegetation cover. At the foot of the hillslopes there is a small creek. Each hillslope plot covers an area of about 33x75 m. In general the hillslopes are planar, steep, and have a similar aspect.

3.1 Geology and soil

The geology of the catchment is of crystalline bedrock with overlain periglacial drift cover (Bachmair and Weiler, 2012). The bedrock is mainly granite but a layer of gneiss runs through the catchment, dividing it into two different parts. Figure 2 shows the geological background of the catchment. The periglacial drift cover evolved from solifluction, cryoturbation and aeolian processes. What is special about underlying periglacial drift cover is the fuzzy boundary between bedrock and soil. Three layers can be identified in the drift cover layer: 1) a basal layer of local bedrock and regolith with high bulk density and compacted, slope-parallel aligned clasts, 2) an intermediate layer with a coarse fraction of finer-sized clasts with varying clast-orientation and bulk density and often with a high content of loess, 3) an upper layer with finest texture and lowest bulk density, predominant for root growth ((Völkel et al., 2001)). Known SSF paths are between the first and second and between the sesond and third layer. Over the drift cover Cambisols has developed on all three hillslopes. The texture is of sandy loam. Bachmair and Weiler (2012) showed that differences in soil characteristics are smaller between hillslopes than profile-wise.

By unpublished data by Astrid Denk (University of Tübingen, 2014) it can be assumed that bedrock is very shallow in the lower part of the mixed forest hillslope. As mentioned above, also recent geologic investigations by Wagner (2014) showed an upcoming rock at the mixed forest hillslope. Additionally, permanent groundwater aquifer were found. Still further investigations are necessary to gain knowledge about bedrock characteristics.

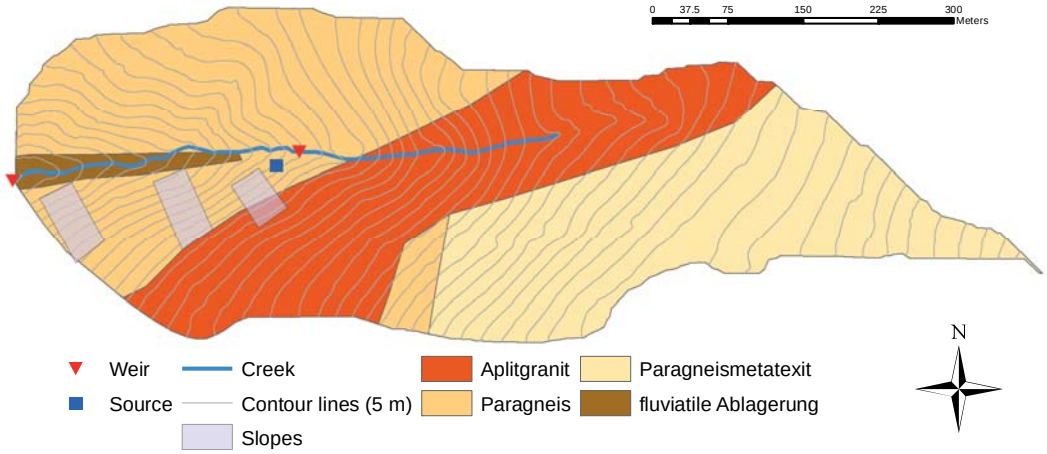

Figure 2: Geological setting of the catchment.

3.2 Land use and vegetation

As mentioned above, the slopes differ in vegetation covers (see figures 3 and 4): grassland, coniferous forest, and mixed forest. The grassland slope is used occasionally for sheep grazing during summer. The conversion to grassland took place about 200 - 300 years ago. At the coniferous forest slope spruce (*Picea abis*), douglas fir (*Pseudotsuga menziesii*), and silver fir (*Abies alba*) dominates. The amount of deadwood and understorey vegetation is high and the ground is covered by a needle layer. Near the creek some sycamore maples (*Acer pseudoplatanus*) and European ashes (*Fraxinus excelsior*) can be found. The mixed forest hillslope is mainly dominated by European beeches (*Fagus sylvatica*) and firs. Some sycamore maples, European ashes and spruces can be found as well. There is almost no understorey vegetation and no deadwood. The ground is covered by a thick layer of partly decomposed beech leaves. The tree ages on both forested hillslopes are about 70 - 100 years (Bachmair, 2012). No recent forestry actions have taken place in recent years - except in the top part.

3.3 Climate

The climate is warm temperate, which is equivalent to the Koeppen-Geiger classification 'Cfb'. Looking at weather data from WBI (weather station of nearby state-run viniculture institute Freiburg) for the time period 2007 - 2011 the mean annual precipitation is 970 mm and the average annual air temperature is 11 °C. Evaparation is highest from May to July. In this time, convective, high-intense storms dominate the precipitation input (Bachmair and Weiler, 2012).

4 Methods and measurements

4.1 Measurement setup

This thesis was planned on the basis of the research done so far in the catchment (see above). Bachmair et al. (2012) installed a sophisticated measurement network consisting, among others, of a catchment outlet, and at each slope a drainage trench and 30 (3 x 10) wells. This setup was supplemented by another weir next to the geological boundary (see figure 2). Besides, a tipping bucket was installed at a perennial source next to the mixed forest slope (see e.g. figure 4). For a better overview of the different sites in the catchment, they are listed below and can be seen in figure 4:

- P: catchment outlet
- M: subcatchment weir at geological boundary
- MQ: mixed forest hillslope source
- N: trench at coniferous forest hillslope
- W: trench at grassland hillslope
- 5, 6, 7: sites along the creek

At the sites 5, 6, 7 water samples were taken and analysed for uranine. No further setup were installed there (except site 5: there is a 5TE-device installed, but data are not used in this thesis).

4.1.1 Setup at the trenches N and W

The trenches at the grassland hillslope W and the coniferous forest hillslope N are 10 m long and about 2 m deep. They drain to a tipping bucket with a 5TE device and an in-situ fluorometer. This setup allows a continuous measurement of discharge, electric conductivity, water temperature and Uranine concentration. The tipping bucket and the 5TE device are logged every 5 min by a EM50 logger. The fluorometer is logged by a Campbell CR1000 logger. As the fluorometer needs a certain volume around the sensor and no external reflection they were installed in a black siphon as it can be seen in figure 5b. Figure 5c shows the installed siphon with the inflow of the trench and the outflow to the tipping bucket. The siphon directs the new water straight under the

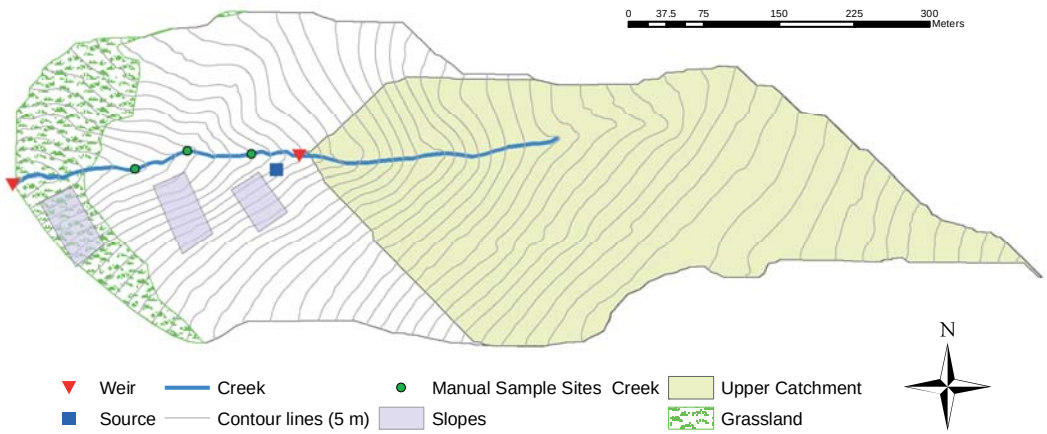

Figure 3: Overview of the catchment and measurement setup.

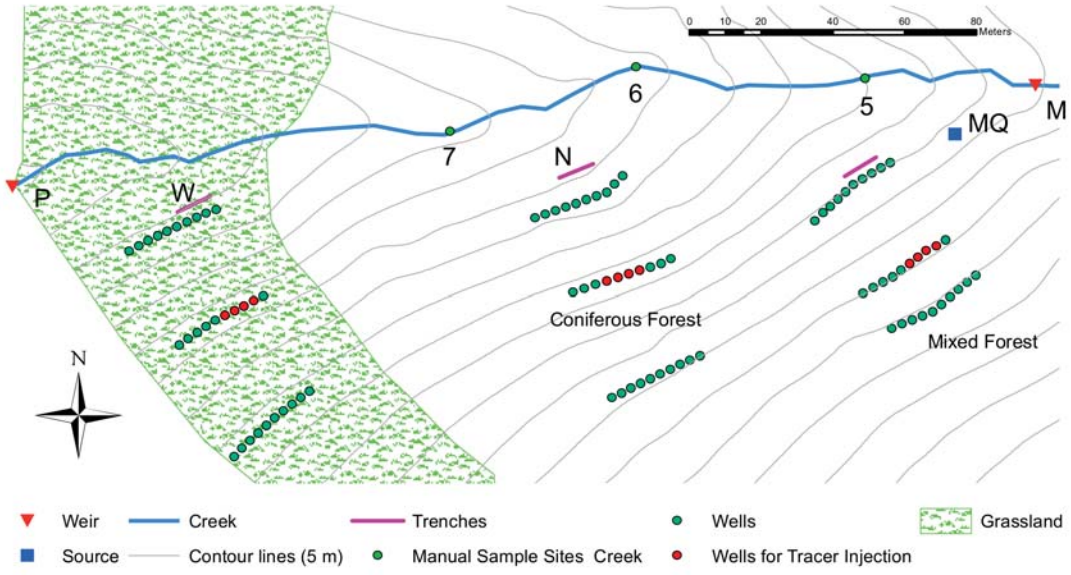

Figure 4: Detailed map of the slopes and the instrumentation including tracer injection wells.

sensor. The overflow/spillover is located above the sensor. This creates a system that ensures that all water passes the sensor and that the sensor is under water at any time. The in-situ fluorometer is a CYCLOPS device (figure 5a). Three different amplifier stages exist: 100 times amplification, 10 times amplification, and 1 time amplification. All signals were recorded and the correct signal was selected in post-processing. The selection of the correct signal depends on the value of the second amplification. Every amplifier stage can give signals in mV from 0 to 3000 mV. If the second stage is less than 300 mV the first signal is correct, if the second stage is above 3000 mV the third stage is correct. In between 300 and 3000 mV of the second stage, the second stage is correct.

(a) Cyclops in-situ fluorometer.

(b) Siphon with 5TE-device and Cyclops fluorometer.

(c) Installed siphon and tipping bucket.

Figure 5: Measurement setup of the Cyclops in-situ fluorometer for uranine concentration measurement at the trenches N and W.

4.1.2 Setup at P, M and MQ

The existing v-notched weir at the catchment outlet (see figure 4P) was additionally equipped with an ISCO autosampler (figure 6a). At the outlet of the upper catchment (see figure 4M) a new v-notched weir was installed (figure 6b). The weir is built of a plastic box with a sharp notch. To avoid leakage, the area upstream the box was sealed with pool liner. An ISCO autosampler was installed at this site, too. Both weirs are equipped with two divers - one measuring the air pressure, one measuring the water pressure including electric conductivity and water temperature. The divers logged data every 5 minutes.

At the mixed forest hillslope another setup was established: As research in the past years has shown, there is almost no discharge in the trench because of upcoming bedrock right above the trench leading the water to the sides of the slope. A perennial source exists upstream and a wet patch of soil downstream. As there is no continuous stream in the wet patch, sampling was concentrated on the source. There, at the mixed forest hillslope source MQ (see figure 4MQ and 6c) a tipping bucket was installed with a small tub and a siphon. Next to the tipping bucket a SIGMA was placed. An

(a) P (b) M (c) MQ

Figure 6: Photographs of the weirs (or tipping bucket in case of MQ) and the autosamplers at (a) the catchment outlet P, (b) the upper sub-catchment MQ and (c) the source at the mixed forest hillslope.

EM50-logger counted the pulses of the tipping bucket and the electric conductivity and water temperature via a 5TE-device every 5 min. The 5TE-device and the hose of the SIGMA were placed in the siphon to ensure water contact at every time. All the auto samplers take samples simultaneously at predefined intervals. During rainfall events the interval varied between 1.5 h and 3 h depending on the intensity and duration of the event. Otherwise, the interval was 24 h. Figure 6 shows the autosamplers and discharge measurement installations.

To gain information about hydrochemistry, isotope composition and in the case of the source and the catchment outlet also to gain information about uranine concentration auto samplers were installed at the two weirs and the source. They sampled the runoff in variable intervals of at least 24 hours up to one hour depending on events. At the weirs auto samplers of the ISCO type were installed. These were able to take 24 samples in total. At the source an auto sampler of the SIGMA type was installed. This device was able to take 24 samples as well. The sample box was closed and well protected against sunlight so that no depletion of uranine could occur. During dry conditions they sampled every 24 hours. When precipitation was forecasted the interval was minimized to 1.5 to 4 hours depending on the expected length of the event. Around 500 ml per sample were collected. These were refilled in 100 ml bottles of amber glass in the field and analysed in the laboratory.

4.1.3 Tracer experiment

Based on a sodium chloride tracer experiment by Ritter (2013), an uranine tracer experiment was conducted to find different flow paths in each of the three hillslopes. Uranine is assumed to be a non-sorptive, conservative tracer that does not underlie biological or mechanical depletion, especially as no uranine experiment has ever been conducted before in this catchment (Leibundgut et al., 2009). The tracer was injected in all three slopes in the four wells marked in figure 4. The selection of the wells for injection was based on Ritter (2013) and adapted to the results. Ritter supposes that

the trenches are supplied more by the wells used in this study. For his investigations he took the first four wells upstream except for the mixed forest slope Where he took the same wells as in this study. In this study the wells were shifted one well downstream. The injection wells are marked in figure 7b by way of example at the grassland hillslope.

Before supplying the tracer to the wells the required mass of uranine was estimated. For this, the annual precipitaion, the amount of precipitation contributing to discharge and the observation time were estimated. The catchment size is known and a mean uranine concentration in the creek at the catchment outlet P of 1 μg/l is assumed. Using equation 1 the mass of uranine for one hillslope is calculated:

$$m(Ur) = \frac{0.001}{365} * OBS * D * A \tag{1}$$

$m(Ur)$ = mass of uranine
OBS = observation period [days]
D = discharge
A = area [m^2]

Table 1 shows the values for the catchment. The result is about 16 g (exact 15.5 g) per hillslope which means 4 g per well - so 3 slopes x 4 wells per slope x 4 g uranine per well = 48 g for the entire catchment. For injection the uranine for each well was solved in 250 ml tab water. The injection was done on 12.05.2015 at 10:30 on the grassland hillslope, at 11:45 on the coniferous forest hillslope and at 12:30 on the mixed forest hillslope.

Table 1: Uranine mass calculation for tracer injection.

annual precipitation	1000 mm = 1 m
proportion to discharge	0.3
catchment area	0.21 km^2 = 210 000 m^2
observation period	90 days
assumed mean uranine concentration	1 μg/l

Before injecting the tracer to a well it was tested with an electric contact gauge if there is water in the well or not. To inject the tracer a hose with a funnel was used (see figure 7c). The hose made it possible to inject the tracer at the bottom of each well. This reduces the loss of tracer at the walls of the wells and minimizes vertical dispersion along the well. After the injection, funnel and hose were flushed with 2 l creek water. This ensured that almost all tracer is injected and nothing remains in the bottles or the funnel or hose and additionally pushed the tracer from the well into the ground.

4.1.4 Manual water samples

Along the creek at the marked sites (5, 6, 7), the weirs P and M and source MQ weekly water samples were taken. There were more sample sites along the creek up to the

source which are irrelevant for this thesis. All samples were analyzed for hydrochemistry and isotope composition as well as for uranine concentration. The sites 5, 6 and 7 are interesting as they lie along the creek but downslope the injection wells of the mixed forest hillslope and the coniferous forest hillslope: site 5 and 6 up- and downstream the geologic rock at the mixed forest slope and site 7 downslope the coniferous forest hillslope (see figure 4). At all sample sites pH value, electric conductivity and water temperature were measured while taking the water sample. Also samples from precipitation at site H from a Hellmann pluviometer were taken and electric conductivity was measured manually before the laboratory analyses. Figure 7a shows the pluviometer and its canopy cover.

(a) Hellmann pluviometer. (b) grassland hillslope. (c) uranine injection.

Figure 7: Impression of the pluviometer, the grassland slope and the tracer injection.

4.2 Laboratory studies

Hydrochemical and isotope values were measured for all water samples. It was tested for these hydrochemical elements: chloride (Cl), nitrite (NO_2), bromide (Br), nitrate (NO_3), sulfate ($SO_4{}^{2-}$), natrium (Na), ammonium (NH_4), kalium (K), magnesium (Mg), and calcium (Ca). The hydrochemical analysis was conducted with an ion chromatograph Dionex ICS-1100. The analysis of water isotopes ($\delta^{18}O$) and deuterium ($\delta^{2}H$) were conducted using a Picarro L2130-i. Samples from site MQ, P and occasionally from sites 5, 6, and 7 were measured for uranine concentration in the spectral fluorometer Elmer LS 50b. All samples were stored cooled in amber glass bottles. For hydrochemical and isotope measurements the sample were filtered by 0.45 μm filter.

4.2.1 Hydrochemistry

To have knowledge about the hydrochemical composition of the water over time allows to see dilution effects during events and may help to identify water sources by comparing samples of different sites. To measure the major ions in the water samples, ion chromatography was used. It was conducted using a Dionex ICS-1100 Chromatogra-

phy System from Thermo Fischer Scientific. For the anions and the cations separated systems exist. In each system the ions in the sample get separated by an eluent with constant (known) concentration and composition. To reduce the conductivity of the eluent the sample passes a suppressor. By passing a detection cell the electric conductivity of the different separated ions is measured. The chromatographs were linked to an auto sampler allowing a run of about 50 samples a time including standard samples. The anions chloride, nitrite, bromide, nitrate and sulfate and as well as the cations sodium, ammonium cation, potassium, magnesium and calcium were measured.

4.2.2 Isotope measurement

Stable isotopes ^{18}O and deuterium were determined for all water samples. Isotopes were measured with a Picarro L2130-i Analyzer using Cavity Ring-Down Spectroscopy (CRDS). The device has a cavity with a laser and a photodetector. The cavity contains three mirrors reflecting 99.999 % of the laser pulse sent by the laser into the cavity. The light circulates in the cavity increasing travel time from a few centimetres (size of the cavity) to more than 20 km. Some light leaks continuously through one of the mirrors to the photodetector measuring the steady light leakage. During a laser pulse, the cavity fills with circulating laser light. The photodetector senses the small amount of light leaking through one of the mirrors producing a light signal proportional to the light intensity in the cavity. Likewise, during the laser pulse, the light intensity increases as well as the signal at the photosensor. When the photodetector signal reaches a threshold the laser pulse is turned off. Now only the light still or already in the cavity circulates and an exponential decay because of steady loss of light is detected. This effect is called ring-down. For an empty cavity this signal depends on the reflectivity of the mirrors.

For a measurement the water sample is vaporized and injected into the cavity. Now not only the reflectivity of the mirror, but also the composition of the vapour affects the signal. The vapour absorbs the light depending on its composition. In general the ring-down will accelerate. By continuous shifting between measuring an empty cavity and a full cavity, precise and quantitative results are obtained. The state of an empty cavity during measurement is simulated by shifting the wavelength to a length where the gas is not absorbing. In fact the laser is tuned to wavelength between the absorption interval. Finally, the measurements are fitted mathematically.

4.2.3 Uranine measurements

Fluorescent tracers are the most important tracers in hydrology. They are easy to handle, have a high sensitivity, a low detection limit, and only small quantities of tracer are needed for field experiments. Uranine is the most fluorescent tracer and the most suitable tracer for groundwater studies (Käss, 2004; Leibundgut et al., 2009). Table 2 shows general specifications of uranine. Especially the low detection limit of 0.001 μg/l and the high solubility of up to 300 g/l make uranine easy to handle in

the field. The photolytic stability has to be seen as a benchmark as numerous studies found different values. It seems to be very difficult to set fixed boundary conditions and the photolytic stability is affected by the material of the sample bottle (best is brown glass) or surrounding radiation (Leibundgut et al., 2009). Of course in the field this is even more difficult especially when uranine is in surface water. There are variable conditions like changing radiation (day-night, shading by trees, turbidity or atmospheric conditions). Table 2 presents the properties of uranine.

Problems with uranine occur with regard to the dependencies of pH and temperature as well as photolytic decay and sorption effects (Wernli, 2003). Another problem with uranine and all fluorescent tracers is a self shadowing effect. This occurs when the concentration is too high and the molecules shadow the fluorescence. If pH and temperature rise, the solubility rises as well. With decreasing pH protons will break up more and more double bonds of the uranine molecule. This leads to a loss of fluorescence. A decreasing pH also leads to an increase of the sorption affinity of the uranine molecule. This may lead to misinterpretation of results e.g. when assuming no hydraulic connection because of no tracer recovery but indeed the tracer is underlying sorption processes. Both effects are reversible (Leibundgut et al., 2009). A non-reversible effect is the photolytic decay. This is a problem when uranine is in surface water. Handling the occurring sorption is quite difficult as different processes like adsorption, absorption, etc. exist. Besides, uranine underlies a chemical and biological degradation. Chemical degradation processes can be oxidation, salination or the conversion to a non-fluorescent derivate. Biological degradation is even more difficult to describe. Here, knowledge is still deficient but it is known that biological degradation exists. The fluorescence intensity is also affected by temperature changes. The intensity is proportional to the temperature and can be described by equation 2 (Leibundgut et al., 2009):

Table 2: Uranine specifications (Käss, 2004; Leibundgut et al., 2009).

Properties	
chemical formula	$C_{20}H_{10}O_5Na_2$
colour index	45350
rel. Fluorescence	100
detection limit [μg/l]	0.001
emission Peak [nm]	516
excitation Peak [nm]	491
$\delta\lambda$	25
solubility [g/l] (20°C)	300
photolytic stability $T_{\frac{1}{2}}$ [h]	11
soil retention [K_d] [ml/g]	0 - 0.4

$$F_s = F * e^{h(T_s - T} \tag{2}$$

F_s = fluorescence at temperature T_s
F = fluorescence at temperature T
T_s = standard temperature [°C]
T = measurement temperature [°C]

The samples were measured with a Perkin Elmer LS 50b spectral fluorometer. A xenon light source stimulates the molecules in the sample and a detector measures the emitted light. To avoid distortion by transmitted light the detector is set up at an angle of 90° to the light direction. A synchronus scan was used to avoid interferences between excitation and emission. A $\delta\lambda$ of 25 nm was used. At the device used in the laboratory the uranine concentration peak occurred at 488.1 nm.

As only at the coniferous forest hillslope and at the grassland hillslope in-situ fluorometers were installed, it was necessary to measure the concentration at the catchment outlet P and the hillslope source MQ manually by measuring the taken water samples in the laboratory. As uranine might have entered the creek at the sites 5, 6, and 7, too, these sites were measured as well. The sites are located straight downslope the injection wells.

As the pH values were far below the value for maximum fluorescence intensity (for detailed values see table 4 in chapter 5) the samples were alkalized with the buffer solution ethylenediaminetetraacetic acid (EDTA). Using EDTA, the pH value was raised to higher than 9. pH did not vary a lot over time so it was assumed that in general every sample is in a similar range. 60 ml of the sample were alkalized with 10 μl EDTA to get an pH >9. By trial and error 10 μl EDTA were found to be the best amount. The dilution of 10 μl to 60 ml sample can be neglected. Before adding EDTA to the samples they were shaked and after adding EDTA the samples were left until sedimentation occur. After adding the EDTA the pH was checked randomly for 3 to 4 samples out of circa 15. Mean pH was around 9.5 $\pm$ 0.3. Subsequently after the pH was checked, each sample was measured at least two times but most were measured three times. The presented values in chapter 5 are mean values of the repeated measurements. The samples were measured at room temperature.

Natural background concentration is probably low. There is no natural or anthropogenic background concentration of uranine. But because the creek water and the slope/trench water can contain suspended sediments causing reflections in the same wavelength as uranine and thus a background reflection receptively concentration. As the background values seem to be quite low and also constant a sophisticated peak separation was renounced. Peak separation can be necessary as the measurements principle is additive. An existing background concentration is added to the real concentration of uranine. To get a tracer induced signal it is necessary to eliminate the background signal from the measured signal.

As already mentioned at site N and W a different measurement setup was chosen. This is already explained.

4.3 Data processing

All data measured in the field were measured in a 5 min interval - except the in-situ fluorometer. They measured in a 30 s interval. The data were checked for consistence,

persistence and plausibility. Failing values were set to NA. All data were aggregated to hourly data (except the precipitation values for the event plots). Hydrochemical and isotope data did not needed any post-processing.

4.3.1 Discharge

The recorded water pressure values of the catchment outlet P and the subcatchment weir M were corrected by the air pressure and calibrated linearly to manual measurements of water height. Using the Thomson weir formular for v-notched weirs (equation 3) the discharge was calculated in l/s for every 5 min interval.

$$Q = 1000 * \frac{8}{15} * \mu * tan(\alpha) * \sqrt{2 * g} * (x - w)^{2.5} \tag{3}$$

Q = discharge [l/s]
μ = discharge constant for weir $0.592 + \frac{0.011 * \mathrm{h}}{\mathrm{w}}$
g = gravity $9.81 \mathrm{m/s^2}$
w = height of weir [m]
h = stowage height [m]
α = half beam width
x = water height [m]

The discharge data were aggregated to hourly data. Outliers were replaced with NA; e.g. values when data were collected from logger. At site M, the weir was jammed at least two times. As an interpolation with electric conductivity and discharge data of the catchment outlet did not give reliable results these values were set NA as well.

Discharge calculation for the hillslope source MQ and both of the trenches W and N was a bit different. As there are tipping buckets installed the output signal is number of tips every 5 min. This signal was re-calculated to discharge with various calibrations for each tipping bucket. The thus calculated discharge was transformed to l/s for the source MQ and l/min for the two trenches W and N. Here, too, outliers were set to NA. The bucket size at site MQ is 92 ml/bucket, at site N 91 ml/bucket and at site W 82 ml/bucket.

Measurement error for the tipping bucket at site MQ is 6.66 %, at site N 0.6 % and at site W 2 %. The error for site P and site M is about 5 %. This error is combined by the error of the barometer, the diver and the manual measurements.

Discharge separation were done using equation 4 (Klaus and Mcdonnell, 2013):

$$F_p = \frac{c_t - c_e}{c_p - c_e} \tag{4}$$

F_p = fraction of pre-event and event water in the stream
c_t = concentration of stream
c_e = concentration in event water
c_p = concentration in pre-event water

The so calculated fraction was multiplied with the discharge to get absolute values for the separation.

For discharge normalization the subcatchment at site M was defined using a DEM. In ArcGIS depressions were filled and flow direction and raster accumulation calculated. Setting the position of the weir the subcatchment were calculated with the watershed function. The entire catchment has an extend of 0.21 km^2; the subcatchment of 0.11 km^2.

4.3.2 Electric conductivity and water temperature

Data for electric conductivity at all sites as well as the water temperature and uranine concentration at site N and W (in the siphons of the trenches) were aggregated from 5 min values to hourly data. Also here outliers were set to NA. The data were corrected by the manual measurements.

4.3.3 Uranine

The in-situ fluorometer which are installed in the trenches at site N and W were calibrated with creek water from the catchment outlet P in the laboratory. No pH correction was done. Equation 5 and 6 show the calibration for site N and site W:

$$c_{UrN} = \frac{U_{fluorometerN} - 1.0062642791}{0.629698754} \tag{5}$$

$$c_{UrW} = \frac{U_{fluorometerW} - 0.836520121355}{0.54193677636} \tag{6}$$

c_{UrN} = concentration of uranine at site N
c_{UrW} = concentration of uranine at site W
$U_{fluorometerN}$ = measured volatge at fluorometer N [mV]
$U_{fluorometerW}$ = measured volatge at fluorometer W [mV]

As the pH value and the water sources have a high variation between the sample sites different calibrations were set up as presented in figure 8. As the calibration was done after the tracer injection water from subcatchment weir M was used. Three calibrations are shown in figure 8: (1) just creek water (BW normal), (2) creek water alkalized with EDTA (BW EDTA), and (3) creek water acidified to pH 6.46 (BW ph6.46). The second calibration was used to calibrate uranine concentration:

$$c_{Ur} = \frac{I_{Ur} - 2.13}{125.23} \tag{7}$$

c_{Ur} = concentration of uranine [μg/l]
I_{Ur} = fluorescence intensity of uranine

Fluorescence intensity of water samples measured in the laboratory were converted with equation 7. The fluorometer in the laboratory has an error of about 1 %. Each sample were measured two to three times. This allowed to calculate a measurement error of 1.19 % for site MQ and 4.36 % for site P.

To calculate the uranine recovery the discharge value at the sample time were multiplied with the measured uranine concentration and the time. The discharge was assumed to be constant until the next sample point. Additionally, an error calculation were done using the error values for discharge and uranine measurement.

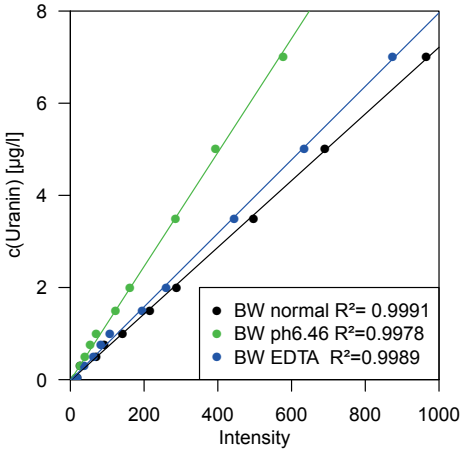

[h]

Figure 8: Uranine calibrations for the Perkin Elmer fluorometer.

4.3.4 Climate data

Climatic data were measured at a climate station close to the catchment until 31.05.2015. Since 01.06.2015 the climatic data from WBI were used as the weather station in Au was damaged. The weather station measured among others air temperature and precipitation amount in a 15 min interval. All data were aggregated to hourly data. A correlation between both air temperature data gave an $R^2 = 0.88$. Also Bachmair (2012) found an error range of 1.2 to 2.5 % for rain duration and around 2 to 13 % for total rainfall and mean intensity comparing both weather stations.

5 Results

To start with, table 3 gives a first overview over the parameters logged at the different sites. The following measurements were conducted: at the sites P (catchment outlet), M (subcatchment weir), and MQ (hillslope source) continuous discharge measurements, autosampling for hydrochemistry, uranine concentration (except for site M) and isotope measurements, electric conductivity and manual measurements were done. At the slope trenches N (coniferous forest) and W (grassland), continuous discharge measurements, electric conductivity, water temperature and continuous uranine concentration were measured. Also manual samples and measurements were conducted. The following results focus on these five sampling sites. Additionally, the climate data and the results of the precipitation samples from Hellmann precipitation collector at site H are presented.

Table 3: Data availability for the monitored sites.

Site	P	M	MQ	N	W	H
Q	x	x	x	x	x	
eC	x	x	x	x	x	x
T	x	x	x	x	x	
pH	x	x	x	x	x	
Isot.	x	x	x	x	x	x
Hyd.Ch.	x	x	x	x	x	
uranine	x		x	x	x	

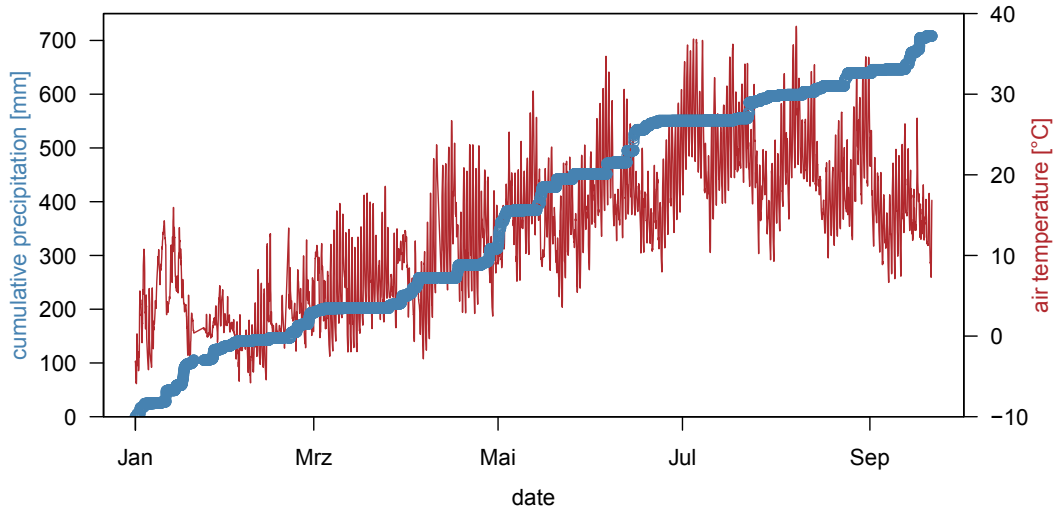

Figure 9: Air temperature and cumulative precipitation at the catchment during the observation period.

To provide an impression of the climatic conditions during the study period figure 9 shows cumulative precipitation and temperature. Since 01.01.2015 708.2 mm of precipitation input to the catchment were recorded. Except for a few days in February, air temperature was positive. July and August were very warm months with daily maxima of air temperatures higher than 38 °C. There were just a few intense precipitation events: one in Febuary/March, one in April, a very large and a smaller one in May, one in June, and one in August. The March event was sampled, whereas the events in April and May could not be sampled as they occurred too suddenly. The June event was sampled again. The event in August was skipped as pre-conditions were very dry, almost no discharge occured in the creek and the forecast was not for a big event. This and the prediction of a quite low event led to the decision not to sample this event.

Table 4: Mean values of manual measurements including absolute and percentage standard deviation.

	eC $[\mu S/cm]$	T_{water} [°**C**]	**pH**
P	140.55	13.57	7.48
	± 38.63	± 5.83	± 0.2
[%]	27.5	43	2.7
W	69.39	14.15	6.76
	± 12.43	± 6.84	± 0.46
[%]	17.9	48.4	6.8
N	129.46	8.65	6.44
	± 10.42	± 3.29	± 0.46
[%]	8.1	38	7.1
H	23.05		
	± 7.63		
[%]	33.1		
7	141.5	13.29	7.55
	± 30.37	± 4.12	±0.19
[%]	21.5	31	2.5
6	140.44	12.87	7.49
	± 30.92	± 3.76	± 0.17
[%]	22	29.2	2.2
5	119.54	10.43	7.54
	± 31.3	± 3.49	± 0.26
[%]	26.2	33.4	3.4
MQ	204.09	9.59	7.00
	± 13.79	± 1.51	± 0.28
[%]	6.8	15.7	4
M	92.3	10.69	7.39
	± 17.26	± 4.77	± 0.22
[%]	18.7	44.6	3

Table 4 presents the mean values including standard errors of manual measurements done once a week. For better comparison the standard error is displayed in percent, too. The measurements were taken in the period from 30.01.15 until 31.08.15. The table shows the range of variability of electric conductivity, water temperature and pH for different sites in the catchment. Looking at the mean values electric conductivity is highest at the source MQ (204 μS/cm) and lowest in the precipitation samples H (23 μS/cm). But also in the grassland trench the mean value is quite low: 69.39 μS/cm. Although site M and 5 are next to each other and both measured in the creek, they differ by almost 26 μS/cm. Downstream site 5 the eC values remain on the level of around 140 μS/cm. The mean water temperature is lowest at the hillslope source MQ and in the coniferous forest hillslope trench N. Except for sites 5 and M, the water temperature in the creek is around 13.5 °C. The water temperature at the grassland hillslope trench is 14.15 °C. The mean pH value is around 7.4 at the sites P, 7, 6, 5, and M. At the trenches N and W the pH is around 6.4 to 6.7. The source MQ has a pH of 7. The variability of the pH values is with 6.8 % respectively 7.1 % highest at W and N and lowest at P, 7 and M with 2.7 %, 2.5

% and 3 %, respectively. Looking at variability, it is very low for pH values in general and for eC and water temperature around 10 to 30 %. MQ shows lowest variability, whereas P, W, N, and M show quite high variability, partly higher than 40 %.

5.1 Hillslope trenches W and N

Figures 10 and 11 show all the measurements from the grassland hillslope W and the coniferous forest hillslope N. They show the discharge and electric conductivity in hourly data for each plot as well as the in situ measurement of the uranine concentration and the water temperature. The time of the tracer injection is marked by a black vertical line.

Figure 10 show the data from the grassland hillslope trench W. Tracer was injected on 12.05.2015 at 10:30. Except for the time during the events at the beginning of March and April there is no significant discharge. During the May event with precipitation of more than 40 mm per day the tipping bucket failed. But for both events in March and April the trench shows a clear response to precipitation input (0.8 l/min, respectively 1.2 l/min). During the few summer events in June and at the end of July almost no response can be seen. Electric conductivity does not show any clear patterns and varies between 55 μS/cm and 120 μS/cm. Uranine concentration shows an increase even before tracer injection and, except for a little increase in mid-July, a recession with daily variation.

Figure 11 shows the data measured at the coniferous forest hillslope trench N. Tracer was injected on 12.05.2015 at 11:45. Discharge is almost ten times higher than at the grassland hillslope trench W. As site W, site N also shows a clear response to precipitation in March and April. The May event could be measured as well. But during the event it was observed that the runoff exceeded the capacity of the tipping bucket. Therefore water passed the tipping bucket without being measured. This led to a steady loss of a few percent of total discharge (5 % according to personal estimation). In June there was a clear response to precipitation. What is noticeable is the shape of discharge peaks: Opposite to W, discharge peaks of N show a slight recession. Electric conductivity varies between 140 μS/cm and 150 μS/cm. EC shows some dilution effects on increasing discharge. Water temperature shows less daily variation than at site W. There is a seasonal increase from 10 to 15 °C. As the installed fluorometer measured even before tracer injection, N seems to have a uranine background concentration of about 0.5 to 1 μS/cm. There is a steady increase of uranine concentration at the beginning of June reaching a plateau of almost 8 μS/cm in mid-June.

5.2 Creek sites P, M and hillslope source MQ

Figures 12 to 14 present the data of sites P, M, and MQ for the whole study period. This is from 05.02.2015 12:00 to 11.08.2015 12:00.

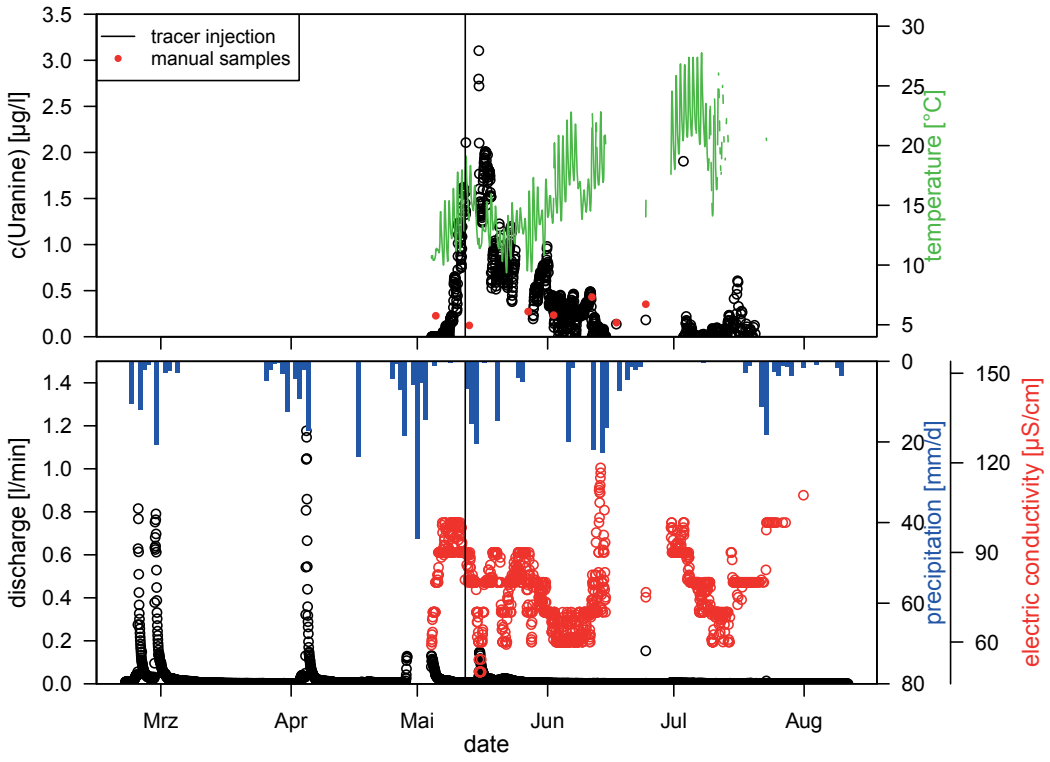

Figure 10: Time series of site W: discharge, electric conductivity, precipitation, uranine concnetration, water temperature in the siphon, uranine concnetration of water samples and tracer injection time.

The upper plot shows the water isotopes ^{18}O and deuterium. Additionally, the isotope values of the precipitation samples and the amount of the samples are shown as well as the point when they were taken. It has to be considered that these samples are composite samples containing a mixture of various precipitation events. The depiction of the water samples and the precipitation amount allows to identify visually if a change in isotope composition in the creek or the source was induced by the precipitation amount or by the isotope composition of the precipitation. If the isotope composition of precipitation differs a lot from the one of the discharge, only a small amount of precipitation water will lead to a change in the isotope composition in the creek. Whereas, if the isotope composition of the precipitation is similar to the one in the creek, and the event is of heavy precipitation, the input of the relative high amount of precipitation water to creek water can lead to a significant change in the isotope composition in the creek. The first case can be seen at the outstanding May event, the second case in mid-April: the event before the biggest rain event.

The central plot shows the timeline of the hydrochemical elements nitrate, sulfate, calcium, chloride, natrium, kalium, and magnesium. Additionally, nitrite, bromide, and ammonium were measured. However, they did not have any or only little and discontinuous values.

The lower plot shows the discharge and the electric conductivity in hourly data aggregated from 5 min values, and additionally the daily precipitation aggregated from

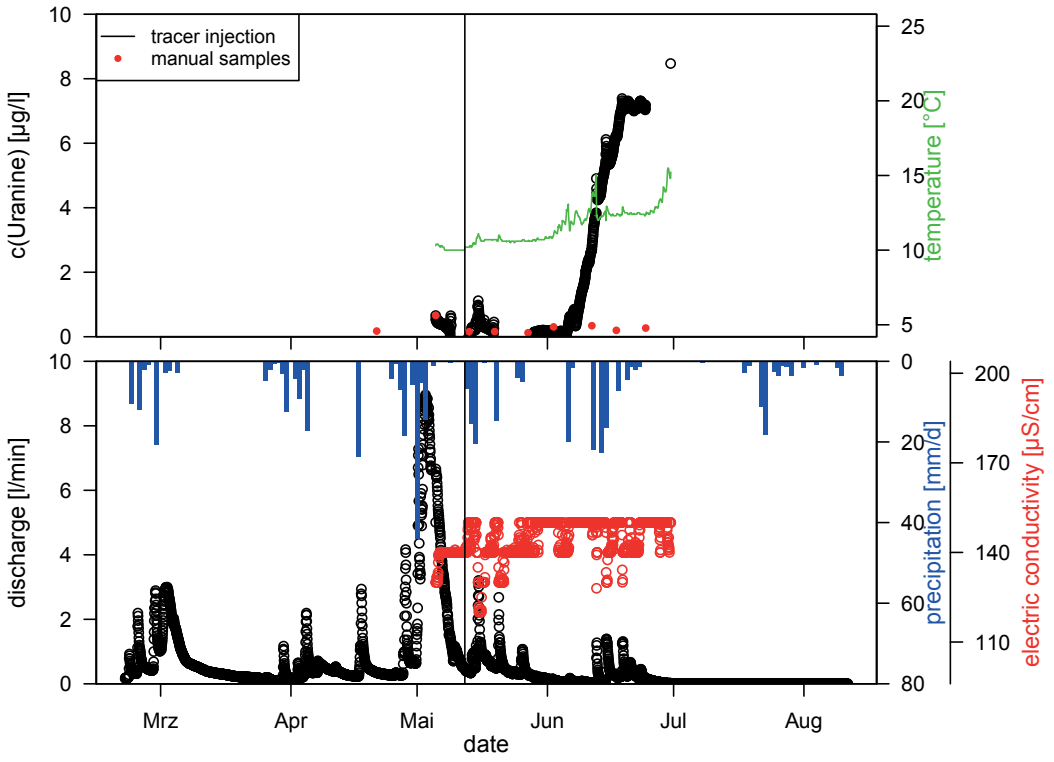

Figure 11: Time series of site N: discharge, electric conductivity, precipitation, uranine concnetration, water temperature in the siphon, uranine concnetration of water samples and tracer injection time.

15 min values (in the figures 15 to 20 showing the events, 15 min values were used).

Figure 12 shows the data from the catchment outlet P. Discharge and electric conductivity react as expected: when discharge increases due to precipitation, electric conductivity decreases. There are two main peaks in the discharge: the first at the beginning of March, the second at the beginning of May. The March event could be sampled and is presented in figure 15. The May event came very suddenly (as can be seen e.g. in the very rapid rise of discharge within a couple of hours). After this huge event no significant discharge peak occurred any more in the study period. Only little rain occurred in May and June. There was almost no rain in July. Together with high temperatures (figure 9), this led to a recession which lasted the whole summer and a very low discharge. During the summer months diurnal variation can be seen clearly. While discharge has decreased steadily from May onwards, electric conductivity was increased almost linearly to around 285 μS/cm.

In accordance with the increasing electric conductivity, the concentration of solutes increases, as well - especially of SO_4 and Ca. To see short time effects during precipitation events the already mentioned March event and an event in mid-June were sampled with an 1.5 h interval (figures 15 and 18). In the March event one can see a dilution effect at least for SO_4. However, NO_3 increases temporally in concentration. This event is described in more detail below. What is noticeable in the entire time line is the steady rise in solute concentration, only interrupted by various smaller precipitation

events.

The isotope plot shows both time series of ^{18}O and deuterium. Additionally, the isotope values of the collected precipitation samples are plotted. The time series over the months show just a little increase from -9.5 ‰ to 8.5 ‰ for ^{18}O and around -70 ‰ to -60 ‰ for deuterium. During precipitation events there is a change depending if the event is more negative or more positive.

Figure 13 is structured like figure 12 but shows the data of the subcatchment weir M. Compared to site P, electric conductivity of site M is generally lower and shows less temporal variability. Electric conductivity shows an almost linear trend from 60 μS/cm to 135 μS/cm. The discharge shows lower variability, too. Besides the maximum discharge of almost 15 l/s the discharge is beneath 5 l/s. Compared to site P the shape of the data is very similar with two main peaks in March and May and a long recession during the whole summer since mid May. What is different is that no diurnal variation can be seen during this recession. In the discharge there are some data gaps due to a jammed weir during events. The blockage was caused by leaves and small branches.

The hydrochemistry plot shows the same dilution effect for SO_4 and an increase of concentration for Ca during events. It is striking that there is no obvious seasonal trend and that Ca concentration is generally a few mg/l lower compared to site P.

The isotopes measured at site M are very similar to site P but seem to be more stable over time.

Figure 14 shows the data of the hillslope source MQ. The discharge is almost four orders of magnitude smaller than at sites M and P. It does not drop below 0.025 l/s. In the March event it reaches a total amount of 0.05 l/s and in the May event even 0.07 l/s. Moreover, the source shows a quite significant recession from mid May until at least the beginning of August. Electric conductivity was not considerably influenced by the events, it is quite constant around 205 μS/cm.

The hydrochemistry shows the highest values of the three figures presented so far. NO_3 reaches almost 28 mg/l, Ca 25 mg/l and SO_4 almost 45 mg/l (in the plot the values are divided by 10 to keep the y-axis in the same scale for all three figures). During the March event (figure 17) some variations are visible. As for the rest, only a smooth variation occurs.

The isotope values show only a little variation during the May event. There seems to be no seasonal trend in the data.

5.2.1 March event

Figures 15 to 17 show one precipitation event in more detail. Each figure represents one site: Figure 15 stands for the catchment outlet P, figure 16 for the subcatchment weir M and figure 17 for the mixed forest hillslope source MQ. The event started on 25.02.2015 at 12:00 and ended on 10.03.2015 at 12:00.

During the event on 27.02.2015 it rained 20.8 mm. After this only single inputs of 1 to 2 mm occurred. The first rain water sample (containing pre-event water) was more

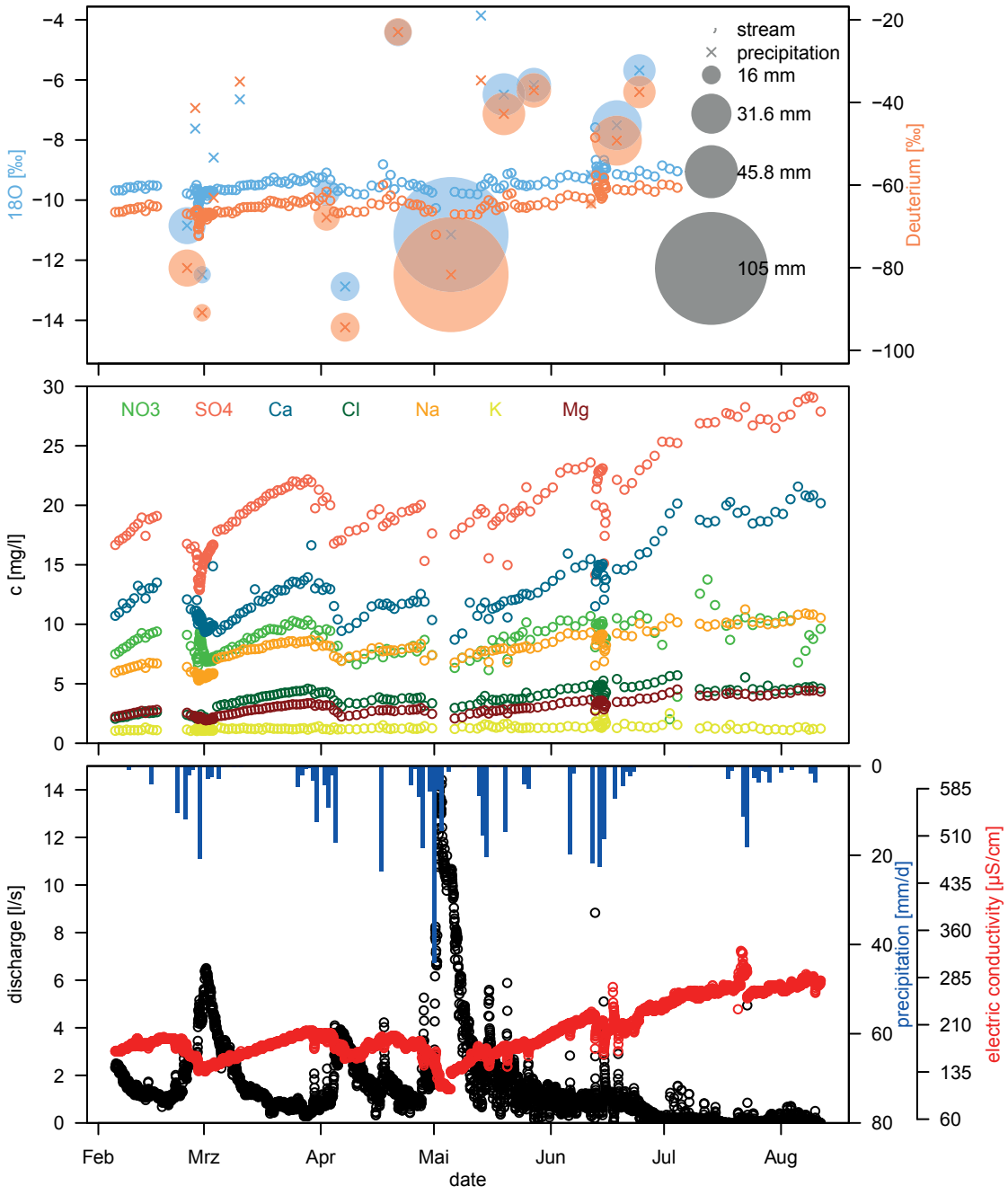

Figure 12: Total time series of site P: discharge, electric conductivity, precipitation, hydrochemistry, water isotopes of discharge and precipitation and precipitation amount.

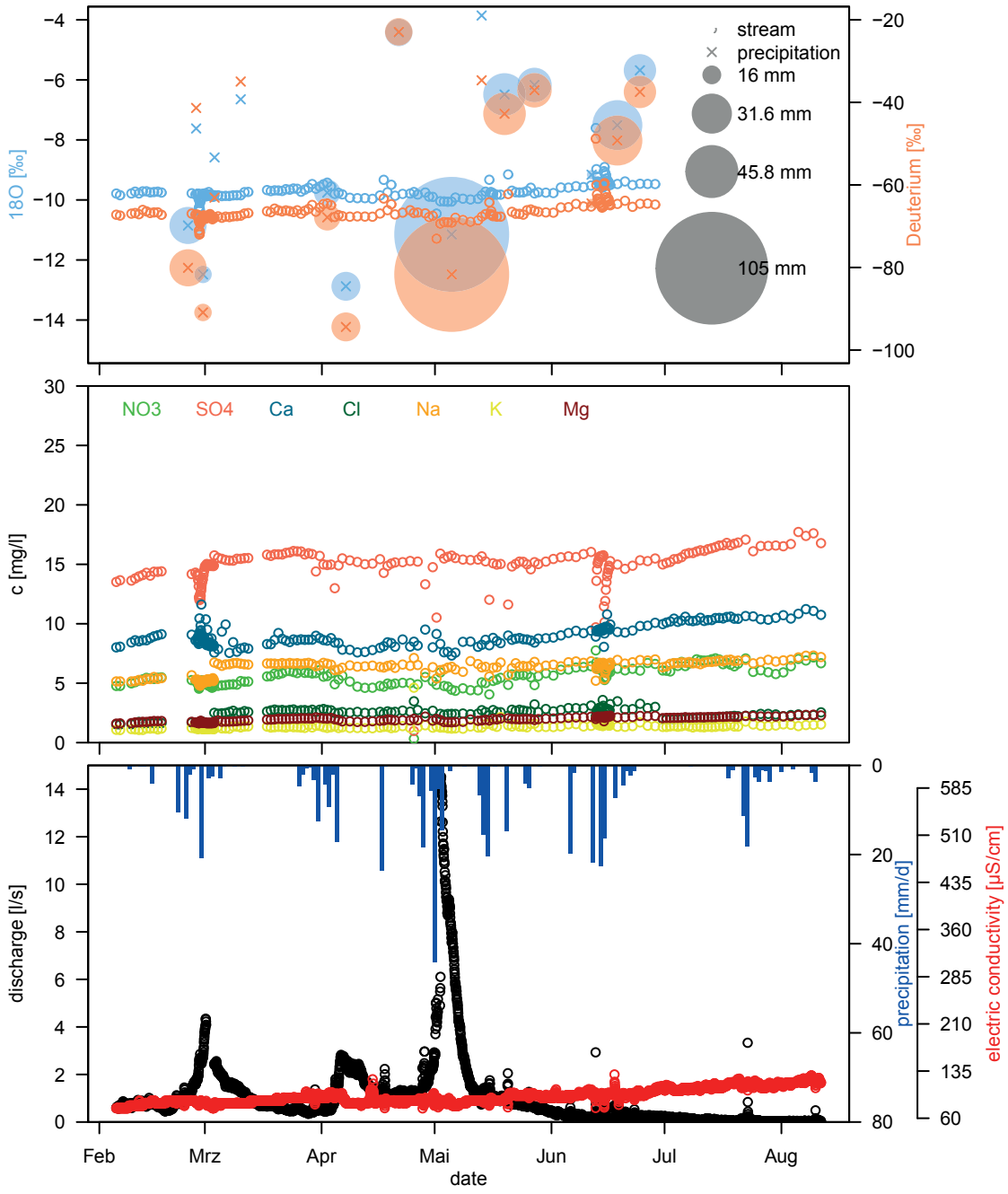

Figure 13: Total time series of site M: discharge, electric conductivity, precipitation, hydrochemistry, water isotopes of discharge and precipitation and precipitation amount.

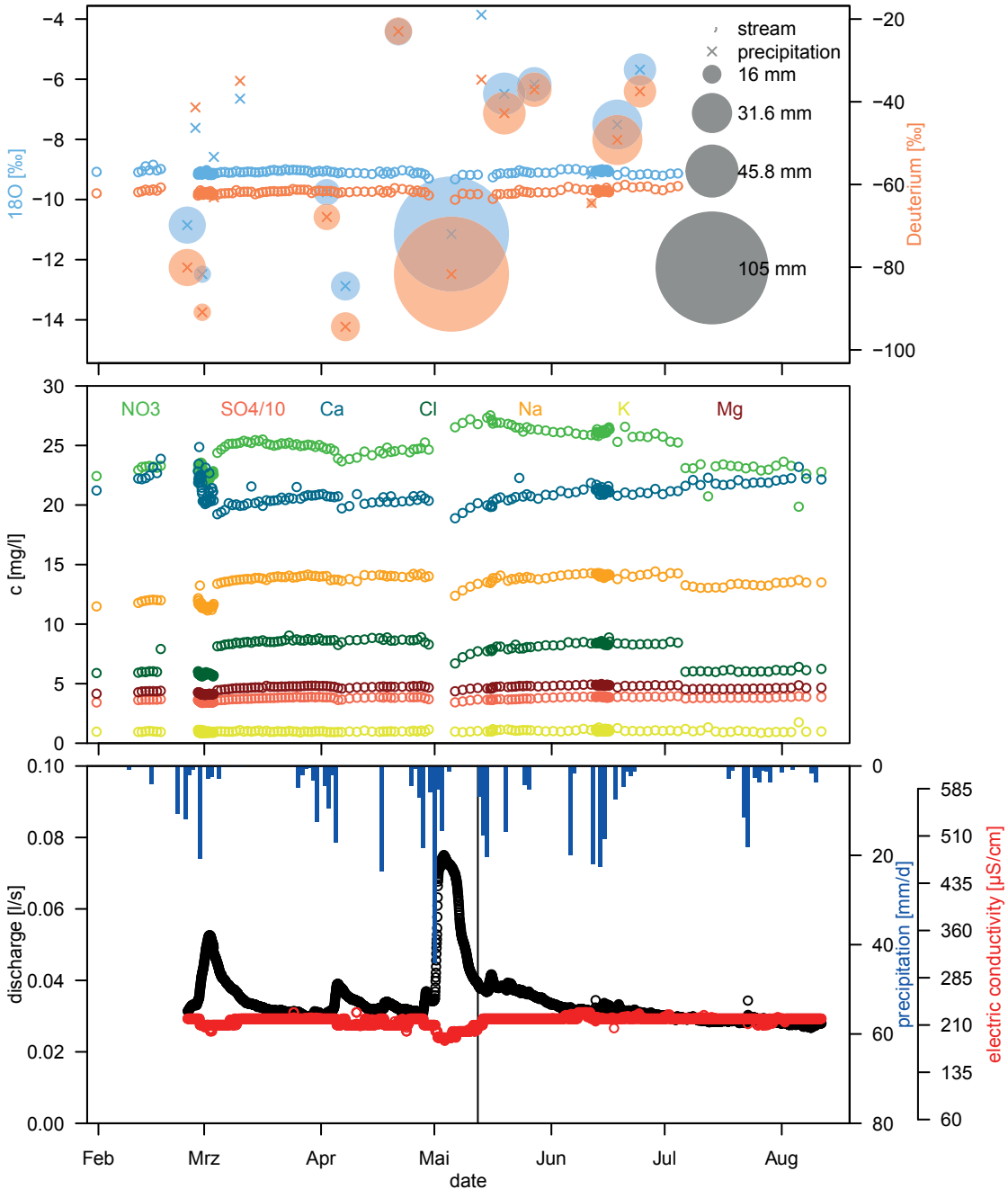

Figure 14: Total time series of site MQ: discharge, electric conductivity, precipitation, hydrochemistry, water isotopes of discharge and precipitation and precipitation amount (black vertical line in the lower plot marks the tracer injection).

positive than the creek water, the second sample (containing the main event) was more negative and the third event (containing most of the small events) was almost at creek water concentration.

Figure 15 shows the catchment outlet P. The discharge shows a double-peak. The first peak occurs on 27.02.2105 with 5 l/s. The second peak occurs two days later on 01.03.2015 with 6.5 l/s. After this peak a recession sets in which lasts longer than the event. The recession is interrupted by a tiny, flat peak on 06.03.2015 with 3.5 l/s. Looking at the electric conductivity a little dip of around 10 μS/cm occurs with the first discharge peak. Afterwards the electric conductivity increases again until it reaches the initial value of around 160 μS/cm. Looking at the hydrochemistry, Mg (2.5 mg/l), K (1 mg/l), Cl (2.5 mg/l), and Na (5.5 mg/l) remain almost constant during the event - only a little smoothing can be detected. Ca is also quite stable but shows some scattering during the event. SO_4 and NO_3 vary a lot during the event. SO_4 values show a dilution effect from almost 17 mg/l to 13 mg/l. After the event a steady increase sets in. Initially NO_3 values show a dilution effect but during the precipitation event an increase occurs from 7 to 10 mg/l. Afterwards the concentration declines steadily. It is important to notice that the only changes occurring in hydrochemistry happen during the first discharge peak. No reaction in hydrochemistry can be seen when the second discharge peak sets in. Isotope values are quite stable as well and just show a negative change during the precipitation event and during the first discharge peak. Almost no changes can be seen during the second peak. ^{18}O is around -9.5 ‰ and deuterium around -65 ‰.

Figure 16 shows the data of site M for the first event. Here again electric conductivity does not show a lot of variability. The discharge data have a gap from 01.03.2015 09:00 to 03.03.2015 11:00. The weir was jammed during this time. There is a slight first peak on the 27.02.2015 and a second one in the time from 01.03.2015 to 03.03.2015. Hydrochemical concentrations are in general a bit lower than at site P. SO_4 shows a very similar reaction. Ca shows a slight increase in concentration and also some scattering. NO_3 stays quite stable and just shows slight variation during the first peak. All changes happen during the event, respectively during the first peak. Also the isotope signal is very similar to site P.

Figure 17 shows the data from the mixed forest hillslope source MQ. The discharge during the event increases from 0.035 to 0.055 l/s and reaches the peak on 02.03.2015. It is a very smooth peak with a long tailing. There is almost no variation in electric conductivity, which is stable around 210 μS/cm. Changes seem to appear in steps but this is due to the coarse resolution of the device. Due to a damaged battery the auto sampler at site MQ missed some samples. The first sample is on 27.02.2015 at 12:00. The values are generally almost more than twice as high as the values from site M and P - except for the K values. For NO_3 and Ca no change can be seen during the event. For Ca there is a slight increase and some scattering. NO_3 varies smoothly between 25 and 23 mg/l. In the isotope signal no change can be detected at all. The values are -9 ‰ for ^{18}O and -61 ‰ for deuterium.

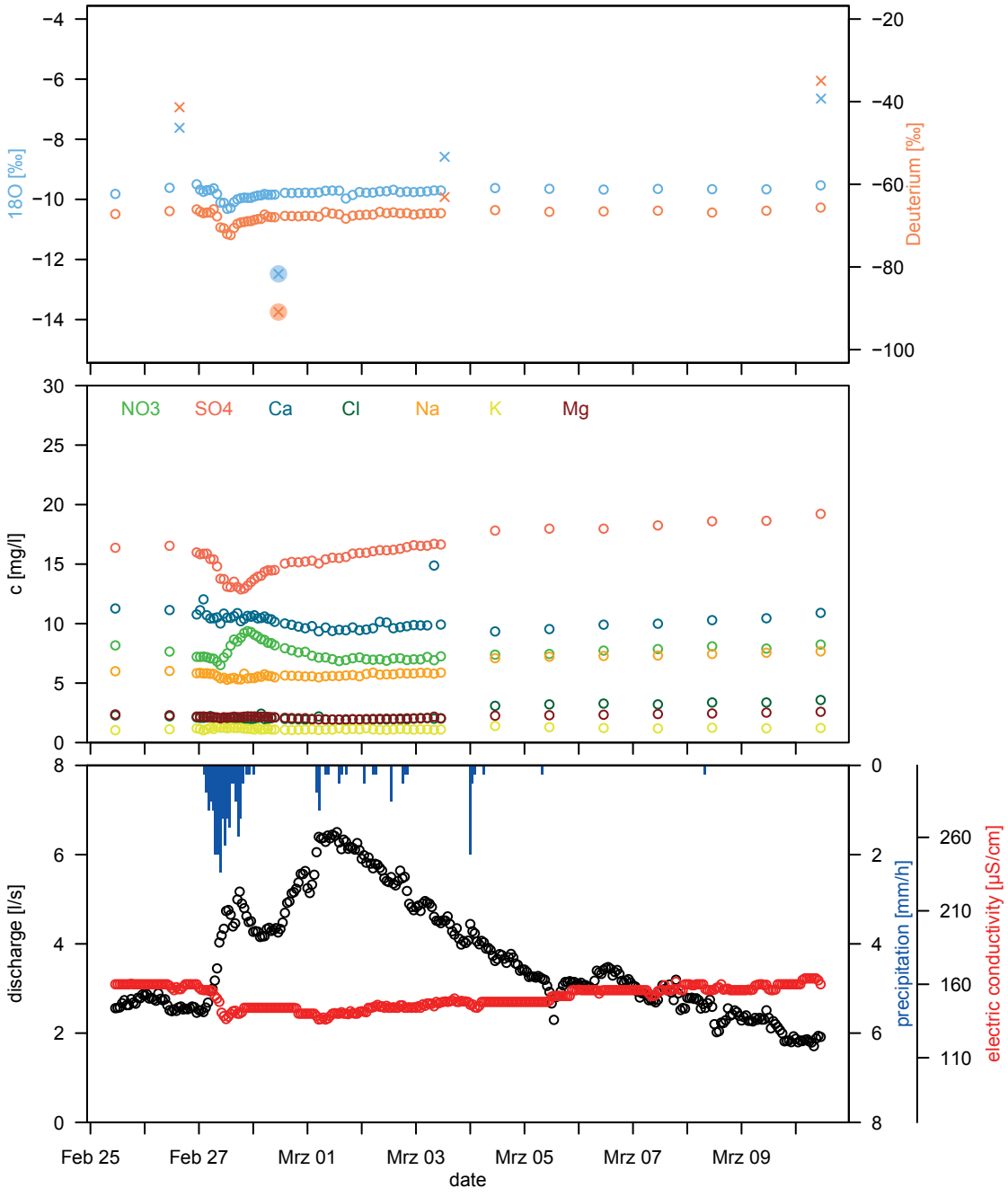

Figure 15: Time series for the March event at site P: discharge, electric conductivity, precipitation, hydrochemistry, water isotopes of discharge and precipitation and precipitation amount (legend for isotope data see figure 12).

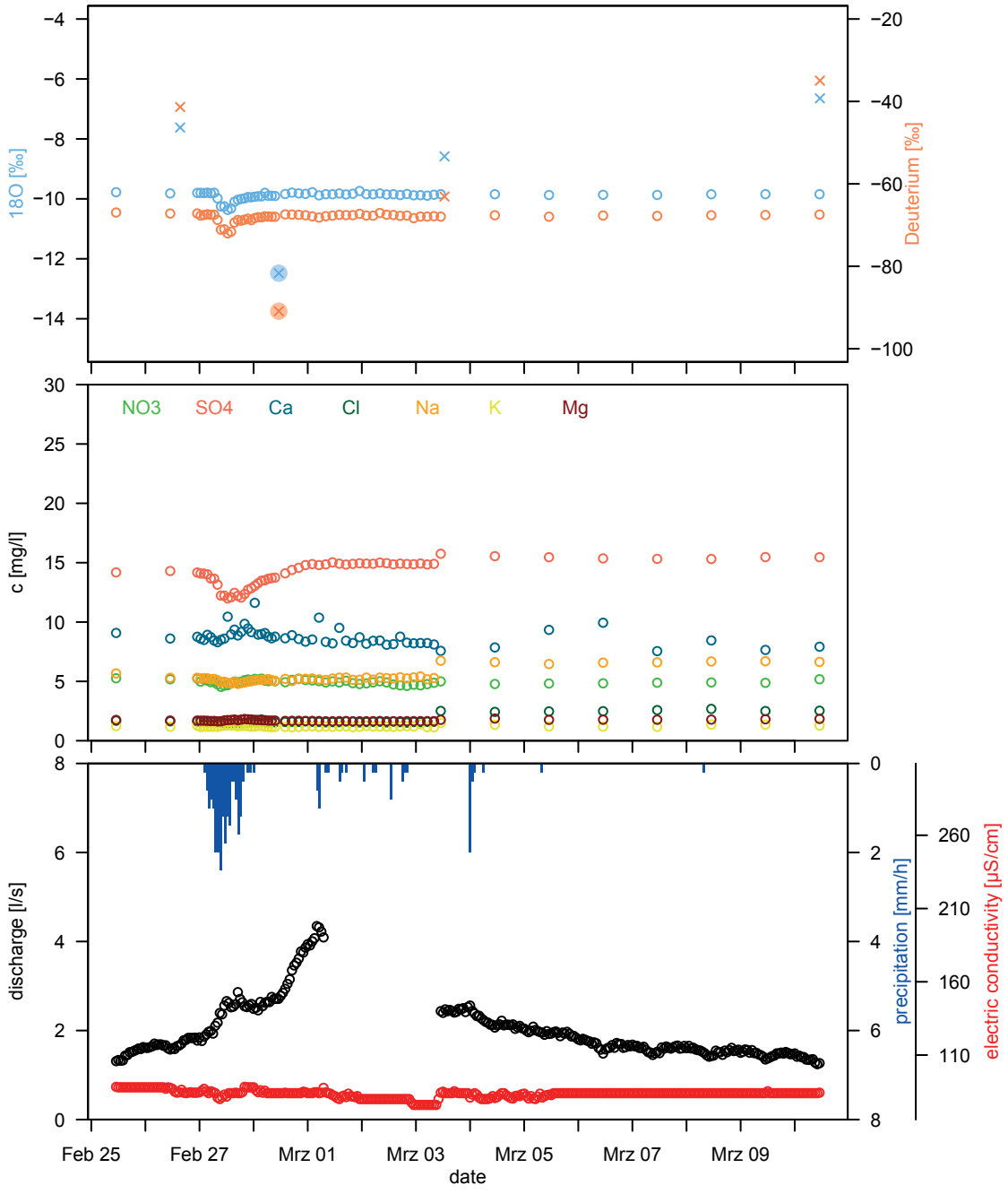

Figure 16: Time series for the March event at site M: discharge, electric conductivity, precipitation, hydrochemistry, water isotopes of discharge and precipitation and precipitation amount (legend for isotope data see figure 12).

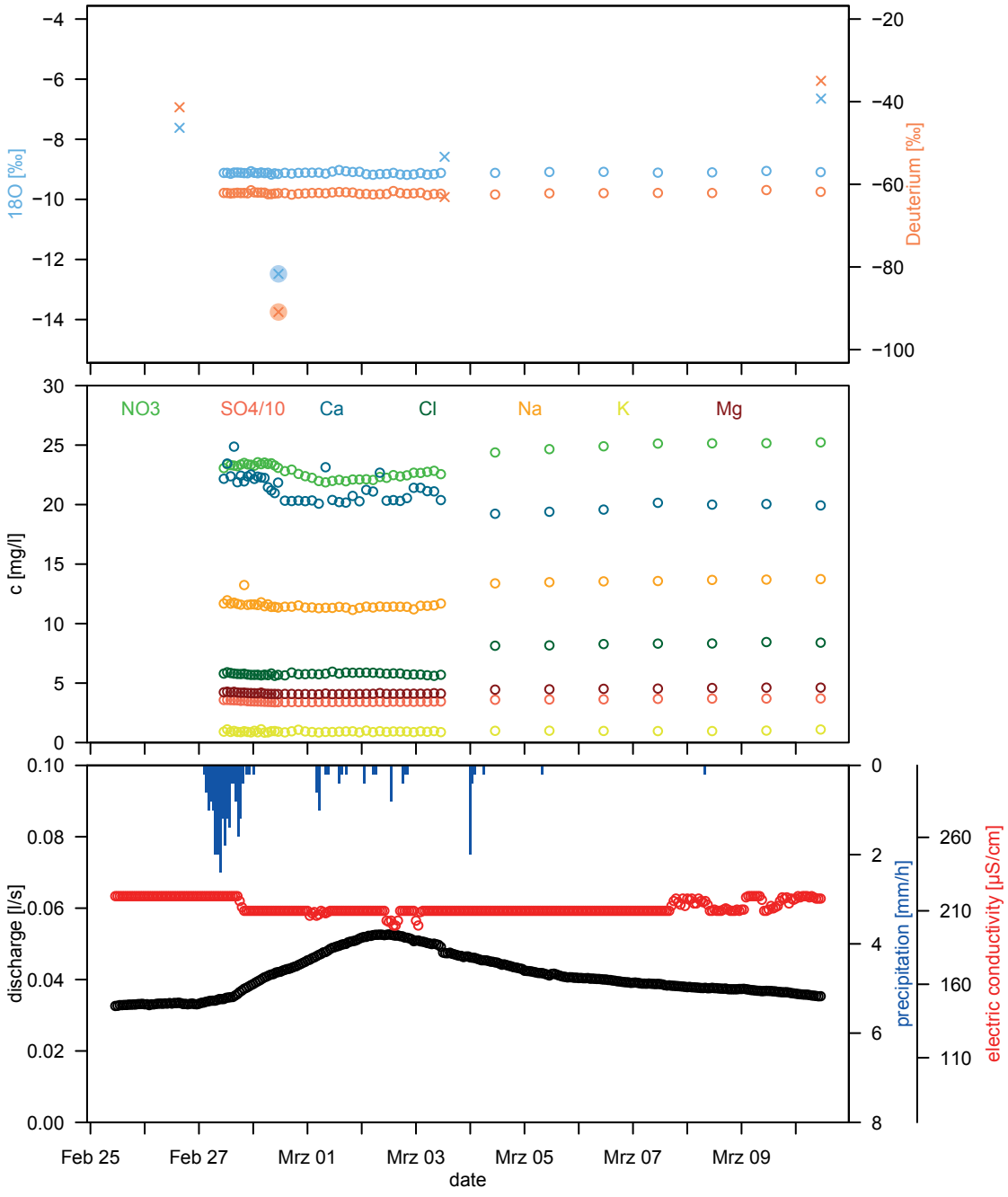

Figure 17: Time series for the March event at site MQ: discharge, electric conductivity, precipitation, hydrochemistry, water isotopes of discharge and precipitation and precipitation amount (legend for isotope data see figure 12).

5.2.2 June event

Figures 18 to 20 show a second event starting on 09.06.2015 at 12:00 and ending on 26.06.2015 at 12:00.

During this second event 61 mm came as input with the first two showers. These are represented by the second precipitation sample. The showers were more positive than the discharge. The little shower afterwards was even more positive. There was a little rain before the event represented by the first sample. This event was of the same concentration as the creek water.

Figure 18 shows the data of site P. The discharge is far lower than during the previous event and clear diurnal variation occurs. The reaction to precipitation input is rapid and short. Discharge increases from 1 to 1.5 l/s up to almost 4 l/s. The peak is very sharp and the tailing very steep and fast. Electric conductivity increased up to 210 μS/cm compared to the first event. It is quite stable but also shows a short but rapid reaction to the precipitation input. After the second rainfall a sudden increase occurs parallel to a decrease of discharge. In electric conductivity no clear diurnal effect can be seen. Compared to event 1 the concentration of solutes is higher this time. Due to inadequate sampling intervals the dilution and especially its recession are sampled badly. Two sudden dilution events can be seen with the first two rainfalls. During the last three very small rain events only a tiny decrease can be observed. But this might be driven by the coarse sample interval. After the first rainfall a big change in the isotope composition can be seen. The values rise from -9 to -7.5 ‰ ^{18}O and from -60 to -50 ‰ deuterium. During the second rainfall only a little increase of around 0.5, respectively 5 ‰ can be seen.

Figure 19 shows the data from site M. The discharge shows no diurnal variation and a very rapid and fast response to rainfall with a very short tailing. After the second rainfall, similarly to site P, a sudden increase of discharge and electric conductivity occurs. Electric conductivity normally is around 100 μS/cm. Hydrochemical concentrations are on the same level as during the first event. The dilution effect is bigger but faster. There is some scattering in Ca. NO_3 shows an increase during the first rainfall but a dilution during the second rainfall. Also Na and Cl react to rainfall. During the second rainfall a light increase of Cl can be observed. Isotope values are very similar to those measured at site P.

Figure 20 shows the data of event 2 for the site MQ. Nothing happens at this site during the event. Electric conductivity is constant at around 220 μS/cm. Discharge is at 0.03 l/s. NO_3 is around 26 mg/l, Ca around 21 mg/l, Na around 15 mg/l Cl around 9 mg/l, Mg around 5 mg/l, SO_4 around 40 mg/l and K around 1 mg/l. Stable isotopes are at -9 ‰ for ^{18}O and at -60 ‰ for deuterium.

5.2.3 Hydrochemistry

Figures 21 to 23 show the hydrochemistry plotted against the discharge for the catchment outlet P, the upper catchment M and the mixed forest hillslope source MQ. Each

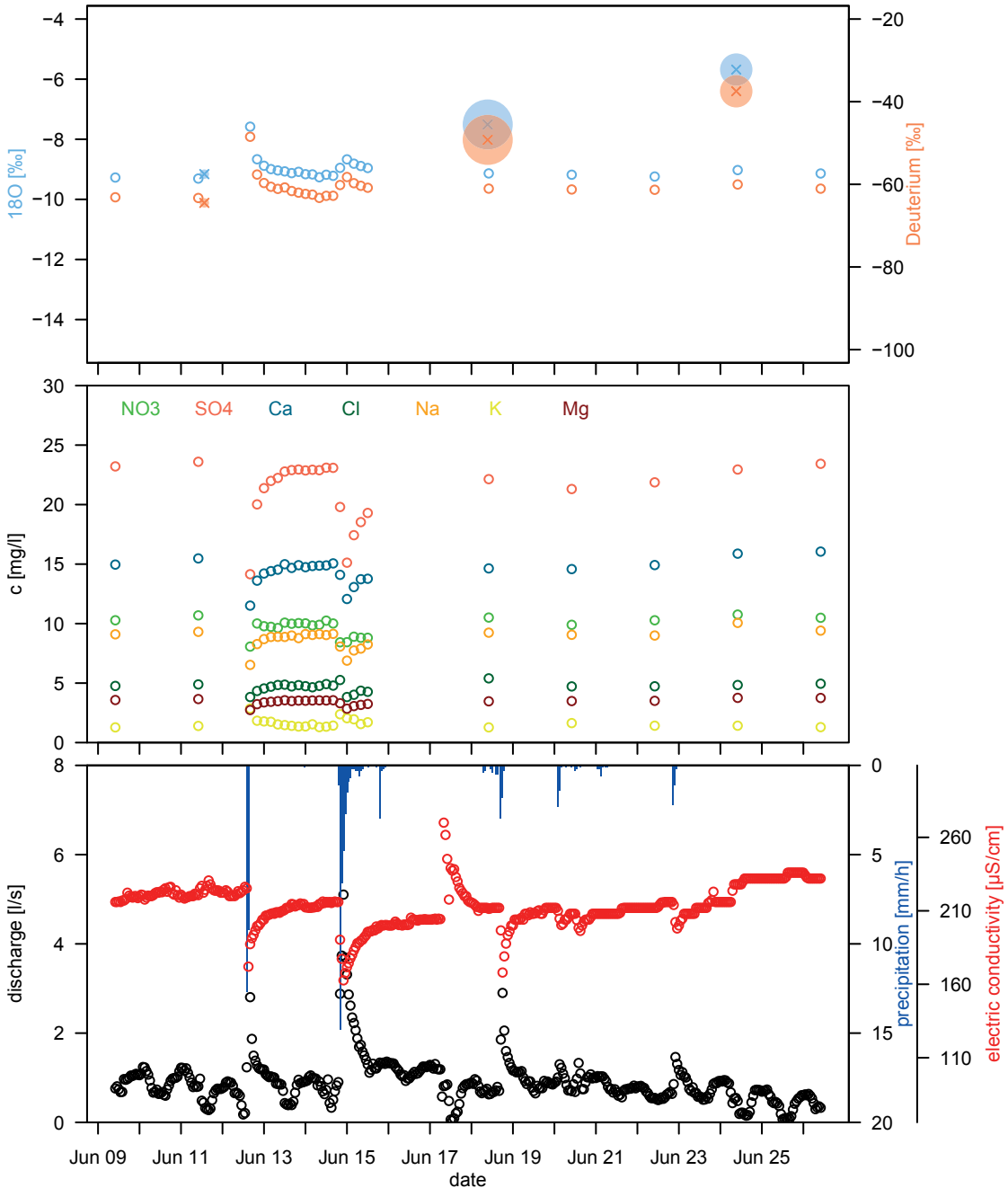

Figure 18: Time series for the June event at site P: discharge, electric conductivity, precipitation, hydrochemistry, water isotopes of discharge and precipitation and precipitation amount (legend for isotope data see figure 12).

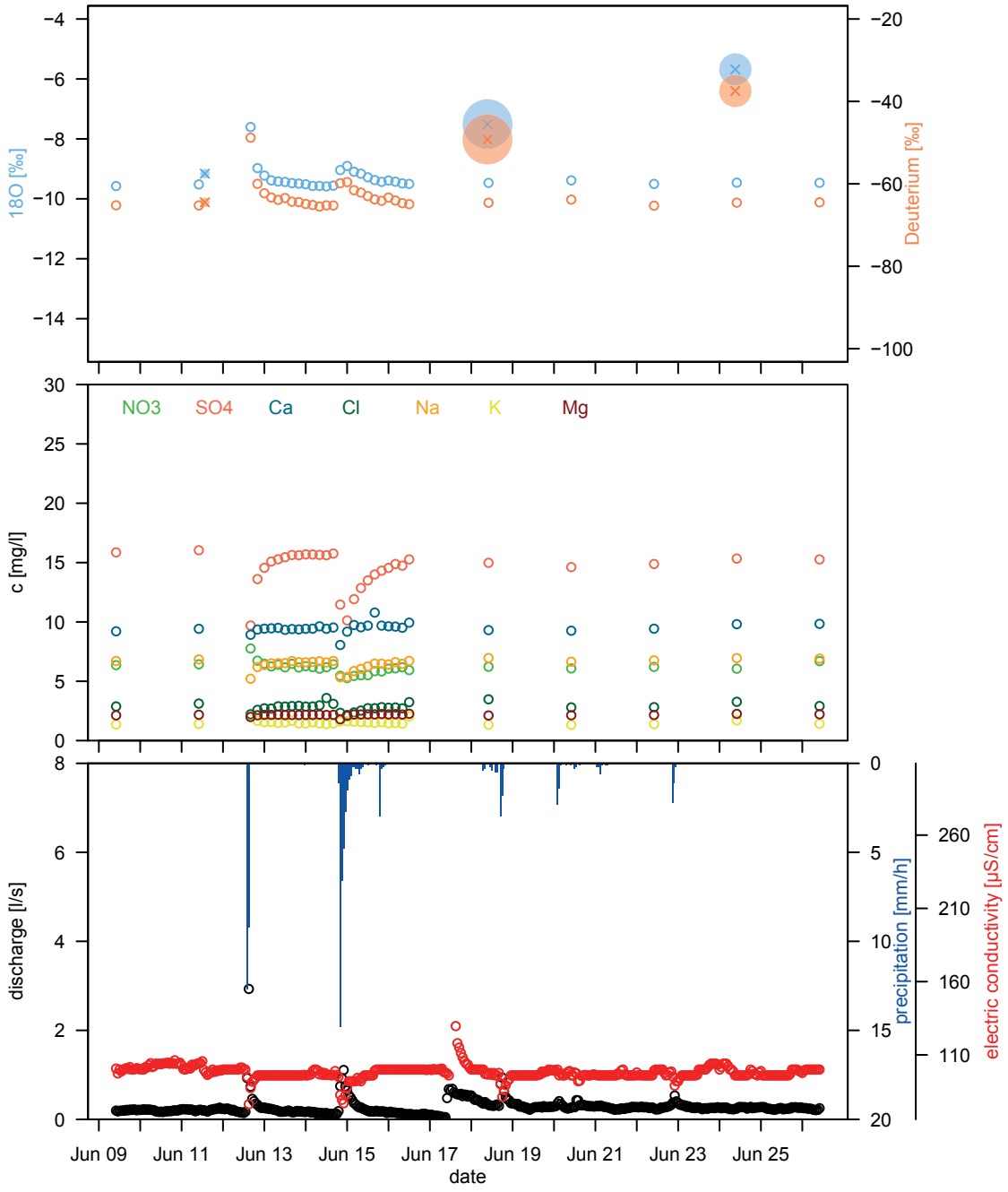

Figure 19: Time series for the June event at site m: discharge, electric conductivity, precipitation, hydrochemistry, water isotopes of discharge and precipitation and precipitation amount (legend for isotope data see figure 12).

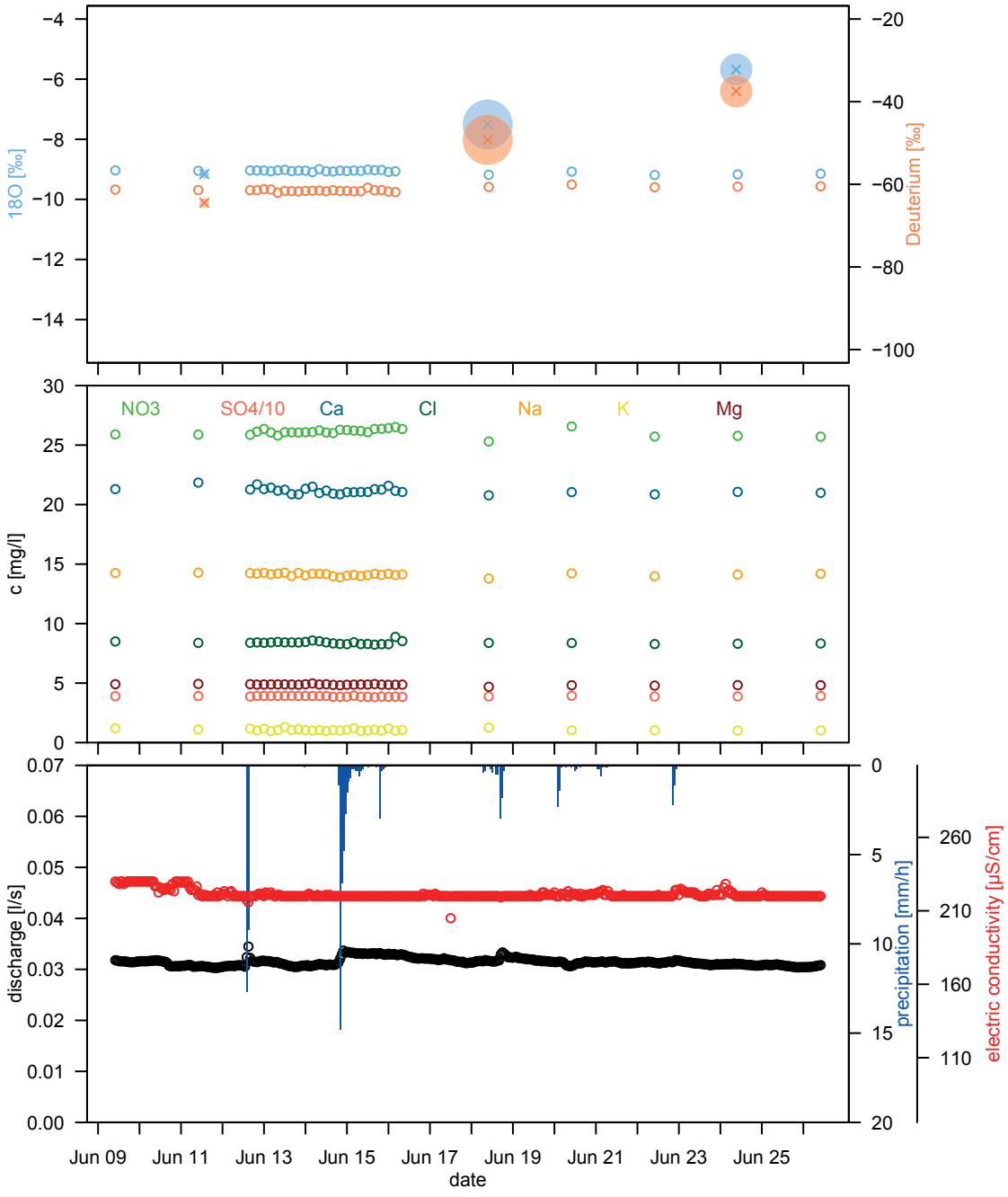

Figure 20: Time series for the June event at site MQ: discharge, electric conductivity, precipitation, hydrochemistry, water isotopes of discharge and precipitation and precipitation amount (legend for isotope data see figure 12).

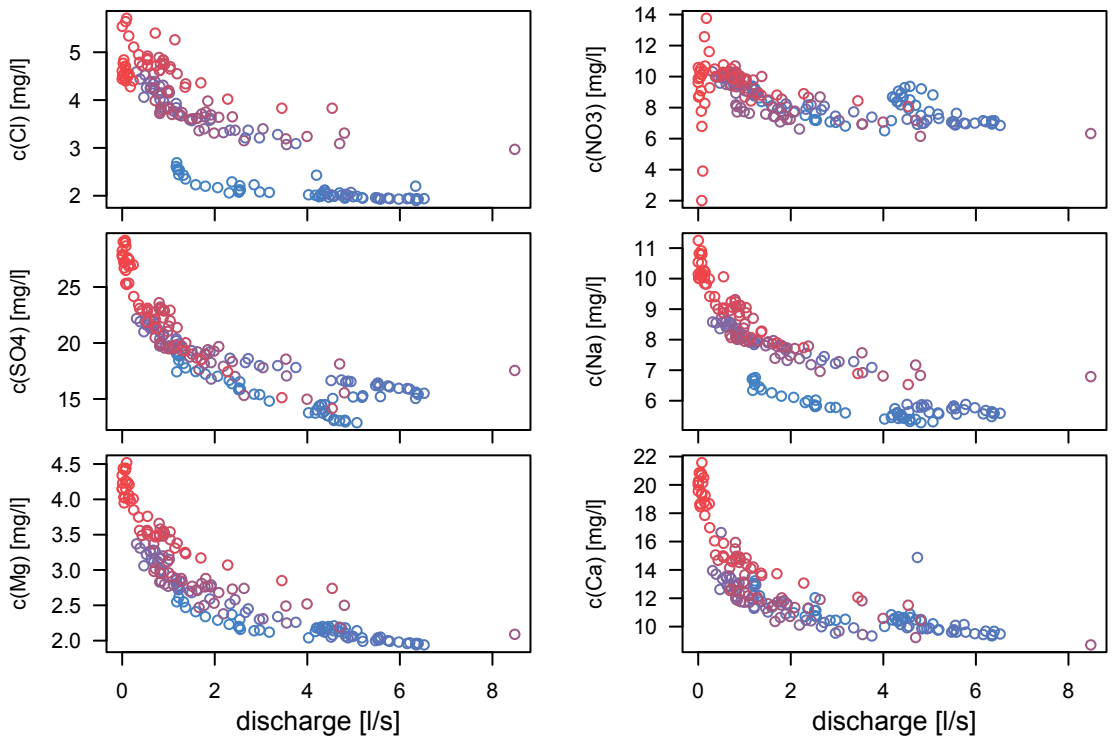

Figure 21: Hydrochemical elements versus discharge for site P. colour shading shows the shift from February (blue) to August (red).

element is plotted separately against the discharge. The elements chloride, nitrate, sulphate, natrium, magnesium and calcium are presented. To get an impression of the change of the ratio between discharge and concentration over time, every measurement point has a certain colour. The colouration starts with blue in February shifting to red until the beginning of August.

Figure 21 presents the catchment outlet P: except for NO_3 all elements form a concave curve. NO_3 seems to remain stable in an interval of 7 to 10 mg/l with changing discharge. This is different with low discharge: Then NO_3 values vary from 2 up to 14 mg/l for nearly the same discharge value. Especially for the elements chloride and sodium some kind of separation can be seen. For the same discharge the concentration is lower early in the year than later. In all plots but maybe best visible in the one showing SO_4 and Mg there is a clear seasonal drift of the curve. Although the time series does not cover an entire year it looks like floods in the spring are different in the hydrochemical composition than during summer.

Figure 22 shows the data of the subcatchment weir M. Here the relationship between discharge and hydrochemical elements look totally different. There is no clear relationship like the curve at site P, but the samples are spread wider. For chloride and for sodium a separation can be seen: same discharge values have different hydrochemical concentrations at different times of the year varying with the seasons.

Figure 23 shows the hydrochemistry plotted against the discharge for site MQ.

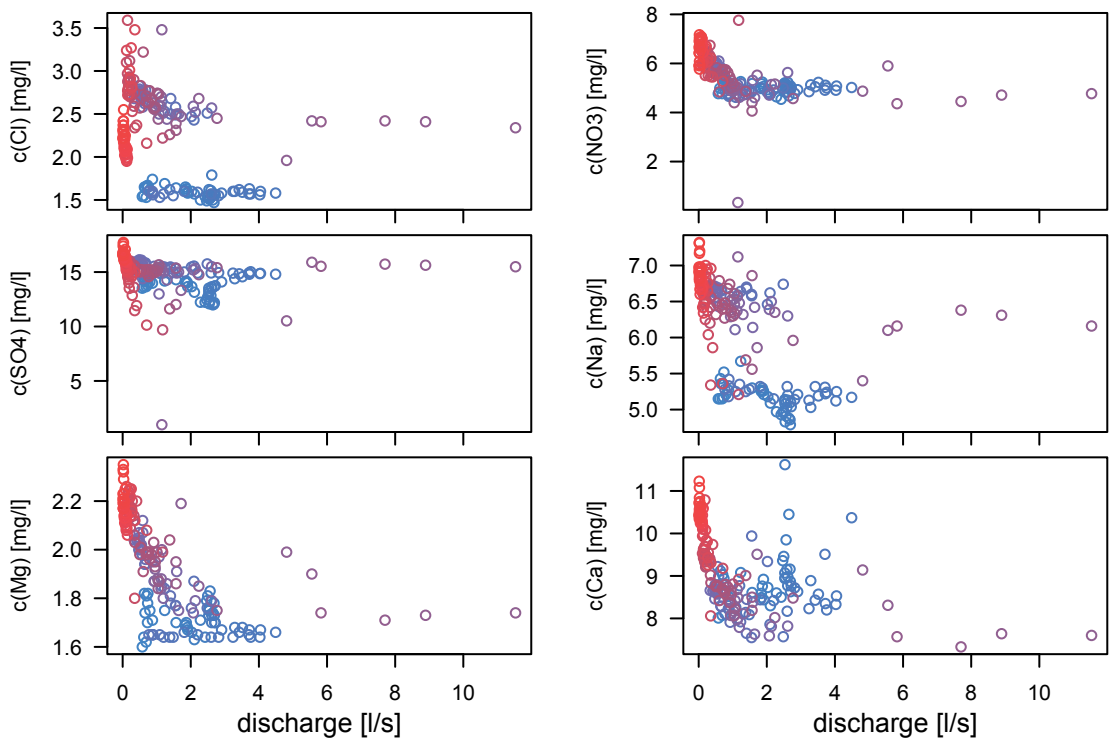

Figure 22: Hydrochemical elements versus discharge for site M. colour shading shows the shift from February (blue) to August (red).

Ca is scattering a lot. There is a trend from higher discharges during spring to lower discharges during summer. The other elements show at least two or three groups not only separated by time (clear differences in colour composition of each group) but also by shape. The blue group (early in the year) is formed like a line resembling the concave curves at site P. The mixed and summer groups are mostly accumulated. The summer group (red, and low discharges) is additionally characterized by (at least slightly) lower concentrations.

5.2.4 Uranine measurements

Figures 24 to 26 present the results of the fluorometer measurements of the auto-sampled water samples in the laboratory. The in-situ data of the installed fluorometer were already presented in figures 10 and 11.

Figure 24 shows the uranine concentration in the source MQ and the catchment outlet P. At site MQ a clear peak in mid-May can be seen. Since then, independent from precipitation input and discharge, a recession has been going on. The uranine concentration of the peak is about 1.1 μS/cm. At the end of August the concentration reaches a minimum of about 0.2 μS/cm. The uranine concentration at the catchment outlet looks much more scattered. There seems to be some steady background concentration and three little peaks with 0.35 μS/cm. The allegedly background concentration is beneath 0.2 μS/cm and never drops below 0.054 μS/cm.

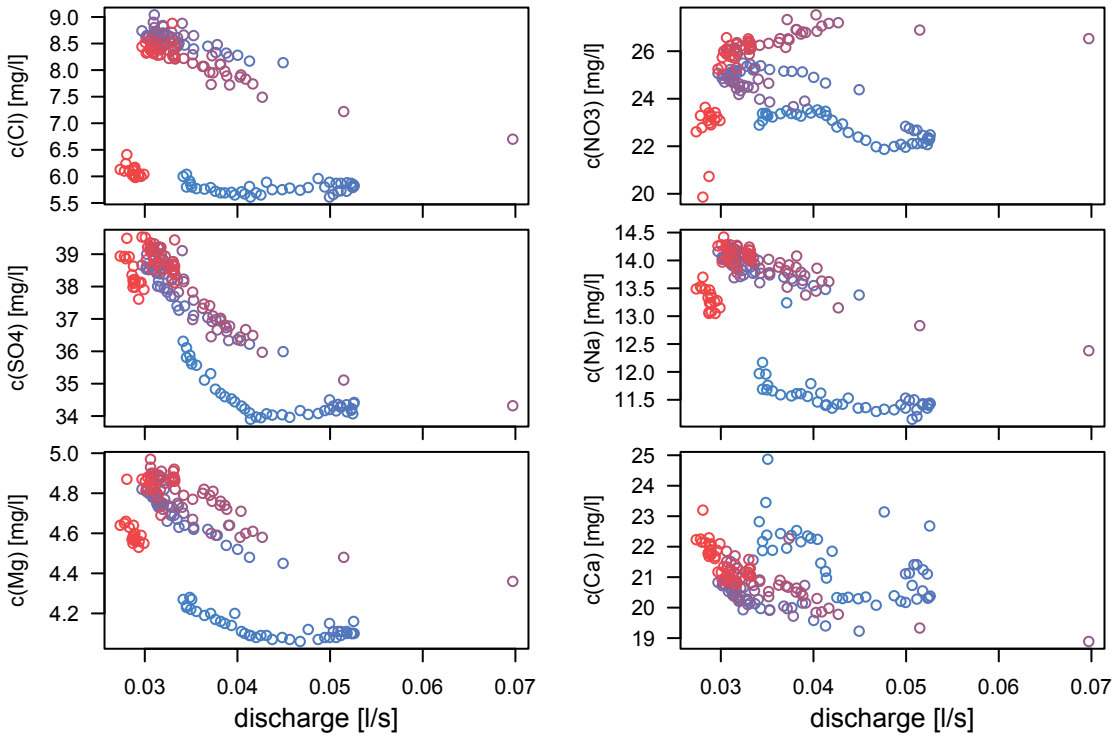

Figure 23: Hydrochemical elements versus discharge for site MQ. colour shading shows the shift from February (blue) to August (red).

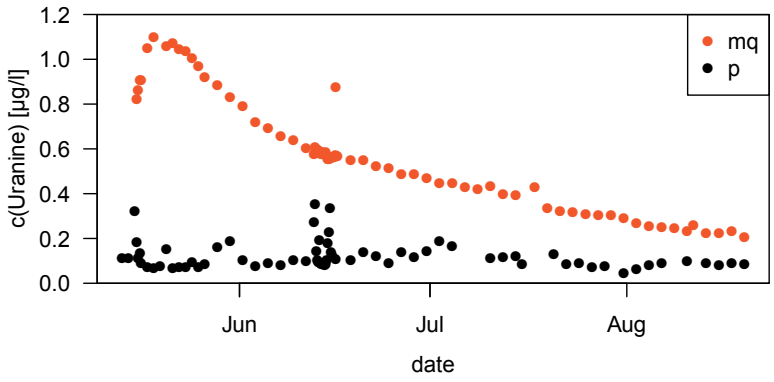

Figure 24: Uranine concentration in the water samples of sites P and MQ.

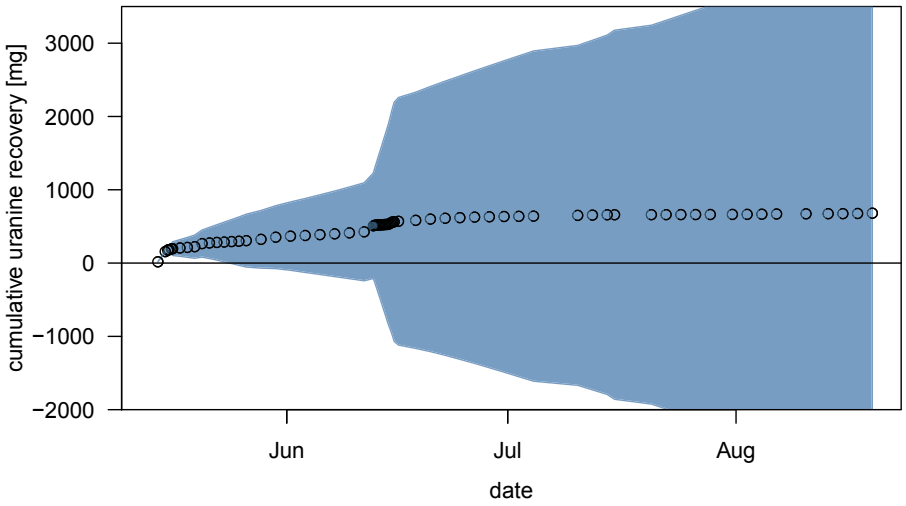

Figure 25: Cumulative uranine recovery at site P including the additive error range.

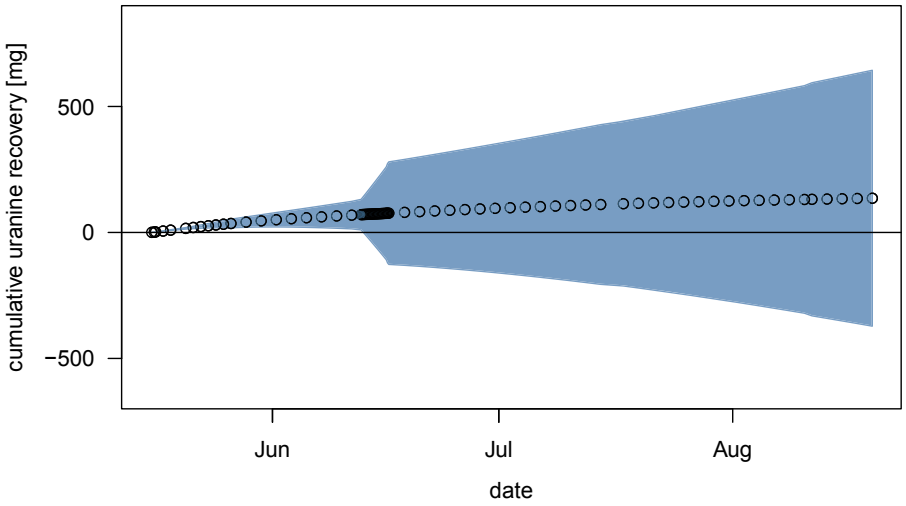

Figure 26: Cumulative uranine recovery at site MQ including the additive error range.

Figure 25 and 26 show the cumulative uranine recovery mass. Figure 25 shows site P, figure 26 shows site MQ. Both figures show the additive error of the measurement in blue. This error results of inaccuracy in discharge and fluorometer measurement and accumulates with each sample regarded for recovery calculation. For both sites the recovery is very flat. So except at the very beginning and very little during the second event some tracer could possibly be recovered at site P. For site MQ most of the recovered tracer was detected at the end of May. Since then the concentration (and discharge) has been decreasing and therefore the recovery mass has not been rising anymore. The error is that big that for both sites it might be possible that no tracer was recovered at all. At site P 680 ± >3000 mg, and at site MQ 135 ± 600 mg of uranine recovery were calculated. To remember: 16 g uranine were injected to each slope.

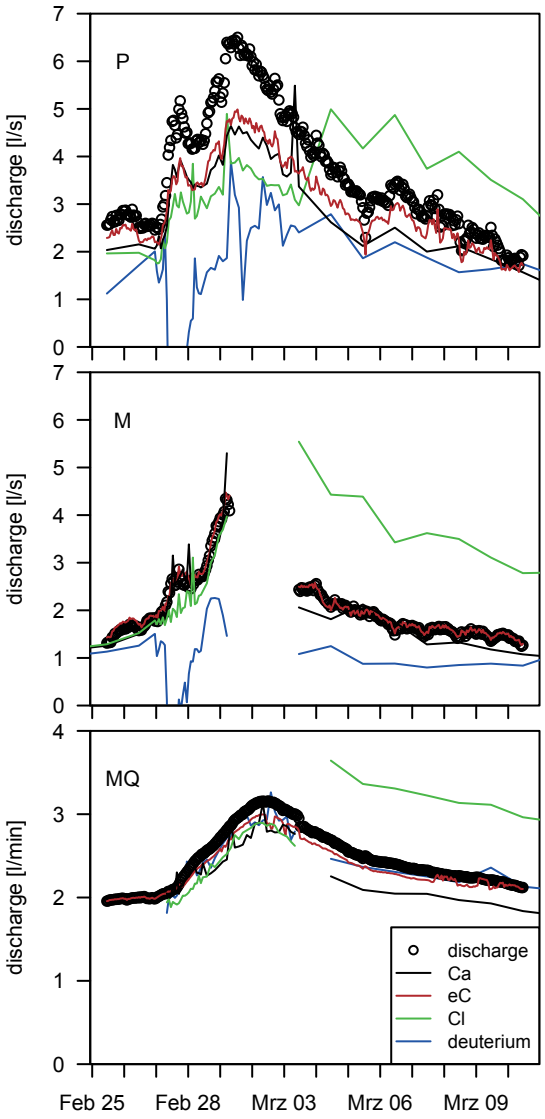

Figure 27: Discharge separation of the March event at the sites P, M and MQ.

5.2.5 Normalized discharge and discharge separation

Figure 27 shows a discharge separation of the sites P, M and MQ using the example of the March event. Ca, electric conductivity, Cl, and deuterium were used for calculating the ratio of event to pre-event water. As mentioned above, site M shows a data gap due to a blocked weir.

For all three sites Cl shows a sudden increase and overestimates the tailing of the event. Deuterium shows a jagged curve. Electric conductivity and Ca fit well to each other and show the highest amount of pre-event water. The different methods show the highest variation at site P and the lowest at site MQ.

Figure 28 presents the normalized discharge for site P and site M. Mostly they

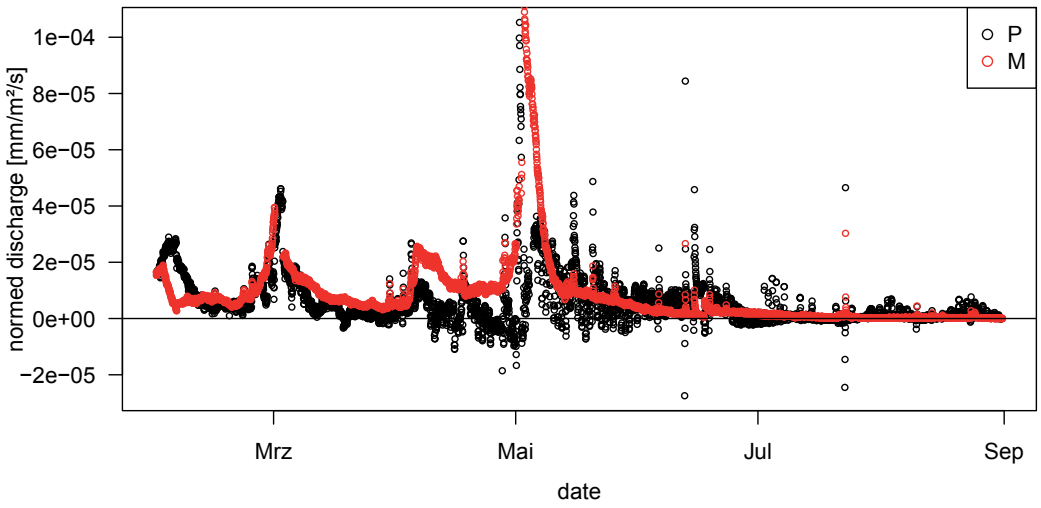

Figure 28: Normalized discharge for sites P and M.

seem to react the same, but two exceptions can be seen: The very first peak and in April. During the very first peak the discharge at site P is higher than at site M and the peak occurrs later. In April the discharge is higher at site M and P even gets negative values. Both time series show a long tailing after the outstanding May event. It is interrupted by single sharp and small peaks. Site P shows some scattering due to diurnal variation, whereas the tailing of site M is quite smooth. This plot shows the extremely low discharge values at the end of the summer, too.

6 Discussion

In the first part, the discussion will focus on the measurement setup and laboratory analysis (particularly the measurement of uranine) including data quality. The second part will link the results to the hypotheses. Finally the results of uranine measurements, hydrochemistry and isotopes are discussed besides the hypotheses.

6.1 Measurement setup

Despite of the unfavourable field work conditions, the selected setup allowed a continuous sampling of tracer concentration, discharge, hydrochemistry, and isotopes at different measurement sites. The data set does not show considerably large gaps. The existing gaps can be ascribed to problems with the equipment, such as damaged batteries, cables or logger problems. One problem occurring with the auto sampler was finding the right start of an event (increasing discharge) and the right sampling interval. This problem could be solved in future studies by automating the start time depending on a threshold for discharge. As the number of samples is limited to 24 bottles, it is necessary to get a good estimation for the duration of the event (including recession) - or, to get the same high resolution for every event, to change bottles after a certain time. This again can cause logistical problems, as each bottle has to be analyzed in the laboratory. The analysis of many samples can become time consuming. Thus, some samples might be analyzed with a significant time delay. During the study period two events were sampled with an acceptable resolution. But many times the sample interval was adapted to forecasted precipitation events which did not occurred in the end. And, otherwise, some precipitation events came suddenly and unpredicted.

To avoid extreme variation of suspended sediment concentration and to reduce the background concentration in the in-situ fluorometer in the trenches it could be helpful to install a fine sieve. This would also help to keep the siphons clean. However, this procedure might require intense maintenance.

At the subcatchment weir M, extreme variation of discharge occurred, especially when discharge was high. This was problematic, as the weir was jammed several times after high intensity precipitation events. In the data this was handled by setting the appropriate values to NA. To improve data quality; two coarse rakes were built a few meters upstream the weir. This reduced the susceptibility of the weir to plugging. After this measure was taken, only one event leading to problems was observed. To get

more information about the circumstances under which the weir is jammed, it could be helpful to install a trailcamera.

6.1.1 Uranine measurement

Calibrating the fluorometer was a sophisticated task. As described in chapter 4, uranine fluorescence is sensitive to pH. Uranine was measured regularly at least at four different sites of the catchment and occasionally at three additional sites. As can be seen in table 4, pH values at the different sites were far below the value for maximum fluorescence (>8 - 8.5) and range about one unit which equals approximately a fluorescence intensity range from 50 to 90 % (Smart and Smith, 1976).

To overcome this problem all samples were alkalized with EDTA to reach a maximum fluorescence intensity (as described in chapter 4). However, one problem remained: the calibration was done after the tracer injection and so it was not possible to do a calibration for each site as possibility exists that tracer was already in the system. However, specific calibrations would have been helpful, as sites can differ in suspended sediment concentration and thus in the background concentration.

As mentioned above, the calibration was done with creek water from site M, so upstream the uranine sample sites. This water has less sediments, thus the given background value is much lower. The background value results from reflections from suspended sediment in the water as the measurement principle is optical and not specific to uranine.

Another problem of calibration could be the temporal variation of pH and suspended sediment concentration. This effect remains unknown here, but should be taken into account in future studies. Filtering samples could be a solution. The temperature dependence of uranine fluorescence should be taken into account as well; especially for site W during summer (see figure 10). Necessary future work is a pH correction for the in-situ measurements. As mentioned, these were calibrated with water from the catchment outlet P.

A specific calibration for each site would be the most accurate way. However, it is difficult to get enough water for calibration at the trenches. Additionally, it should be considered in further studies that another tracer has to be used, as uranine is now already present in the system.

6.2 Results

For the following discussion it is important to keep in mind that the field work took place during a particularly dry and hot summer. There were just a few intense precipitation events: one in Febuary/March, one in April, a very large and a smaller one in May, one in June, and one in August. The March event was sampled, whereas the events in April and May could not be sampled as they occurred too suddenly. The June event was sampled. The event in August was skipped as pre-conditions were very dry, almost

no discharge occured in the creek and the forecast was not for a big event. This and the prediction of a quite low event led to the decision not to sample this event. After the tracer injection in mid-May just three events occured - and not a single significant discharge peak at all. At the same time air temperature started to rise up to more than 30 °C. To describe the settings of the field work in short, it can be noted that spring was characterized by high precipitation. High summer temperatures set in at about the time of the tracer injection. Besides continously high temperatures, the summer was very dry. This lead to high evapotranspiration, extremely low discharge and dry soils. Those conditions hindered transport and mobilization of the tracer, and made its detection and SSF sampling difficult.

6.2.1 Hypotheses

Although some knowledge about the mixed forest hillslope could be gained (see 6.2.5), no specific flow paths could be detected. As mentioned above, the tracer experiments did not work as expected because of a long summer drought. As explained in chapter 2, tracer experiments are essential for investigating the hypotheses. Hypotheses 1 and 2 explain the double-peak events by different flowpaths along the hillslope. To gain knowledge about this the tracer experiment was designed. As discussed below the design was quite well done but one important thing was missing this summer: subsurface flow - or rain. To transport the tracer water flow and therefore rain is necessary. But as can be seen in figures 10 and 11 almost no rain and thus no discharge occurred. So the tracer experiment failed and therefore nothing can be said about hypotheses 1 and 2. Additionally, only one double-peak event occurred during the study time. For hypothesis 3 (double-peak events are driven by the geologic boundary layer) some evidence was found to discard it: in March one event was observed and sampled very well (event 1), but no other double-peak event occurred. The observed double-peak event occurred both at site P and site M. This indicates that it is not the geologic boundary layer effects the double-peak by a different reaction of both of the catchments parts. This contrasts with the quite different behaviour in hydrochemistry where site M is much more similar to the hillslope source MQ (figures 21 to 23 and chapter 6.2.3) . Site M seems to be, similarly to the source MQ, a mainly groundwater fed site, whereas site P has at least some components of event water. But both have the similar discharge characteristics and both subcatchments behave almost the same. What is different is that site M does not have any inflows but local source water and site P, additionally to this is also influenced by inflow of M and the slopes.

Hypotheses 1 and 2 need further investigations and a lot more rain. However, the summer draught was positive for two things: gaining knowledge for longtime uranine background concentration for site P and MQ. Additionally some nice observations could be measured at site MQ (see below).

6.2.2 Uranine results

Looking at the results of uranine measurement, four sites are of main interest: W, N, P, and MQ.

The only site showing a seemingly clear peak is MQ with 1.1 μg/l. The fact that this peak occurs at the 18.05.2015 - thus seven days after injection - can be considered a quick reaction. Especially when taking into account that the start of the peak probably reached the source a couple of days earlier. The measurements started on 16.05.2015, four days after the injection. The delay was caused by a damaged battery. At this time uranine concentration had already reached a level of 0.8 μg/l. Looking at the tailing, the natural background might be at or even below 0.2 μg/l. One possibility for this quick reaction is an already active subsurface flow path transporting some tracer to the source. As precipitation in May was quite high, the SSF path network might still have been at least partly active when the tracer was injected. During transport time the flow path stopped and drained due to higher temperatures, subsequently higher evaporation and low precipitation.

At site P the uranine concentration signal is a lot more diverse. There are three tiny, sharp peaks related to precipitation events. Between the events, scattering of measured values made it hard to quantify background concentration. This is because much more suspended sediment with varying concentration was in the water and samples were not filtered before measurement. The background concentration is probably up to 0.2 μg/l. The uranine concentration peaks are not necessarily due to uranine in the creek as they might be caused by higher suspended sediment concentrations flushed in with rising discharge.

Looking at the data of the in-situ fluorometer at site N and site W, both seem to have a peak. The data recorded at both sites show special characteristics: At site W the peak starts even before tracer injection (see figure 10). The recession lasts until mid-June and shows no reaction to discharge (which is in fact almost zero). Opposite to this, the concentration of manual samples is almost constant with a value of around 0.3 μg/l. The peak might be caused by higher background concentration due to suspended sediments. The sediments might have been brought into the system by the huge May event. As mentioned, this event was not measured but observed. The recession shows daily variations that seem to correlate inversely with air temperature. Site N shows a sudden but steady rise of uranine concentration until a plateau is reached. This rising is independent from precipitation or discharge, which was very low. Manual samples do not show this rise. In fact, after the mid-June event the siphon was cleaned due to dry conditions. While cleaning the siphon, shiny, small worms were found on the ground of the siphon. These worms probably caused a higher reflection. However, this could not be proven. After the siphon was cleaned and re-installed no discharge occurred until the end of the field work. But here again the manual samples indicate that no tracer could have been detected. Important at these two sites for future investigations is the higher sorption effect by lower pH.

Looking at the tracer recovery at site P and MQ the amounts are tiny compared to injection mass, while the additive error is all the greater. This gives rise to doubts if there is any tracer recovery at all. As the error fan of site P is excessively large, the recovery of 680 mg out of 48 expected g very low and the background signal very scattered, it is assumed that no tracer passed this site. Additionally, it has to be noticed that no further measures were taken to reduce the background than doing the calibration with creek water. Same is valid for site MQ, but as the signal is quite distinct here and the error fan is not that excessively large it can be stated that at least very little tracer could be recovered. A better dealing with the background concentration is recommended for further investigations. This could be done either by subtracting a certain value of every value assuming a constant background or by a peak separation for every measurement. The first method is probably fine with site MQ as the discharge do not react fast and almost no suspended sediments are solved. From observations while taking the samples it can be stated that site P shows much more suspended sediments and much more variation, too. For this site the second method is recommended.

Although nothing or just very little uranine could be detected so far and the tracer experiment did not bring the desired information for subsurface flow paths, some helpful results for future studies were gained. General setup and injection mass seem to be well designed. It seems that the background concentrations are very low and the calculated mean concentration of 1 μg/l is appropriate. If tracer breakthrough should occur at some time in the future, additional measurements at the following sites would be of interest: 5, 6, 7 and the wells in the first well row. The sites were measured occasionally in this study but no tracer could be measured. For future studies, especially concerning the tracer breakthrough of the current experiment, it is important to take degradation and sorption effects of uranine into account. E.g. Wienhöfer et al. (2009) had very low recovery rates as well and attributed sorption and degradation effects for this.

6.2.3 Hydrochemistry and isotopes

Hydrochemical figures 21 to 23 show some seasonal loop effect and a kind of separation or grouping effect. The grouping effect may be caused by different reservoirs reacting to different precipitation inputs and/or antecedent conditions. The grouping increases in the course of time. This can be discussed best in figure 23. The figure shows (1) a distinct blue group with low values of solute concentration for a quite large variation of discharge during spring, (2) a mixed color group with lower discharge but higher concentration of solute during early summer, and (3) a group in late summer with very low discharge and low to medium solute concentration.

The loop effect can be seen best in figure 21 showing the hydrochemistry of site P. This loop occurring within the concave curve might be a hysteresis effect caused by different pre-conditions like saturation of the soil or soil temperature (frozen top layer?).

Differences in the figures 21 to 23 could be explained by different runoff composi-

tions. Site MQ is a groundwater source as can be seen in figure 27 and as discussed later. Site P has a large amount of groundwater baseflow but is much more sensible to event water. Site M is in between those two sites.

Looking at the event plots, the different reactions of site MQ compared to site P and site M are striking. In the first event site MQ shows only a smooth reaction in discharge and hydrochemistry, in the second event there is almost no reaction. The low reaction to precipitation, the high solute concentration values as well as the steady isotope signal in both events are clear indicators for a groundwater source. As there is at least some tracer recovery, the reservoir is at least at 2 m depth or even deeper (tracer might have infiltrated to deeper soil layers).

The invariable isotopic signal at the sites P, M and MQ is in contrast to the variability in the isotopic signal of the precipitation, which indicates that large parts of the catchment are groundwater or pre-event driven. Again this can also be seen in discharge separation.

Further investigations are necessary. At least it would be of interest what happens during autumn and winter and if the patterns still can be seen when plotting a whole year, or if there are the same or different pattern in the two half-years. Differences might occur because of precipitation characteristics, vegetation, weather/climate (evaporation).

6.2.4 Discharge

Comparing discharge of site M and site P, site P seems to be a lot more influenced by daily variation: The summer recession is very smooth for site M and a significant daily amplitude in site P. This amplitude gets smoother during summer. Normalized discharge shows - beside the mentioned daily effect - almost the same runoff behaviour for both sites.

Discharge at the mixed forest hillslope source MQ shows a very steady signal and constant electric conductivity. This indicates a groundwater source. Also the smooth and slow reaction to input signals (precipitation) can be seen as evidence for a groundwater source. That the discharge was higher at MQ at the end of August compared to site P is another clear indicator for a long dry summer. In this case (without normalizing discharges, just by the total amount) obviously water was lost. The water probably evaporated or trickled away into the dry ground.

The coniferous forest hillslope trench N and the grassland hillslope trench W show both the expected reaction: site W has lower discharge than site N and site N shows longer recession after peaks. This could lead to the assumption of a temporally active short-time reservoir, whereas at site W just subsurface flow paths dominate the discharge at the trenches. Further investigations have to analyse hydrochemistry and water isotopes in more detail to gain knowledge about the water composition at the trenches.

Looking at the results of discharge separation, four parameters were used: eC, Cl,

Ca, and deuterium. Generally all parameters seem to have worked out, but there are some things to be aware of: (1) Cl overestimates the tailing of all three sites. (2) deuterium shows a jagged graph. (3) eC shows the highest resolution. (4) resolution of Cl, Ca and deuterium is high during peak but coarse in the tailing. The problem of overestimating and the problem of isotope scattering might be caused by the very coarse sample interval of precipitation samples and the fact that theses samples contain water of various events.

Discharge separation with eC gives the highest pre-event amount. It is the separation with the highest resolution due to continuous measurement. Following this separation site M and MQ are almost completely supplied by pre-event water or groundwater. This clearly emphazises the ideas of runoff generation so far. Discharge separation with Ca is very similar to the one with eC but more coarse due to the measurement intervals of the auto sampler.

Better results could be provided for discharge separation with isotopes by a higher sample interval for precipitation samples. All samples are mixed samples of different events. Changes in and between events are not taken into account and sudden changes appear. For future analysis Ca concentration and electric conductivity seem to be the best.

6.2.5 Conceptual model for mixed forest hillslope source MQ

High solute concentrations and constant isotope signal imply that the source is fed by a well-mixed groundwater reservoir. Maybe this reservoir is dammed by the upcoming rock boulder at the mixed forest hillslope. This has a residence time of more than a year - probably at least around 3 to 5 years - to ensure a complete mixture and so a constant isotope signal. Several factors could be seen as an indicator for different components in the reservoir: the varying relationship of solute concentration and discharge as well as the described grouping and looping effects. During winter and spring the reservoir is filled up. This means that water can flow in upper soil or ground layers. These are more fractured than deeper layers, as the degree of fracture decreases with depth. This allows higher flow velocities of water and results in lower residence time. A lower residence time means less time for the water to solve minerals from the rock and thus results in lower solute concentration. During early summer, when the vegetation period starts, air temperatures rise and precipitation decreases, the reservoir drains and water level drops. Now the water flows through less fractured areas with lower flow velocities and higher residence time. Thus solute concentrations are higher and discharge is lower. During (late) summer or during very dry periods the reservoir is already empty and water drains only from very unfractured areas. But this do would mean even higher solute concentration. But the opposite was observed. Maybe this is caused by water that entered the deeper zones but had a lesser residence time due to the extreme empty aquifer.

The observed grouping pattern could be described by several theories. The de-

scribed phenomena could be a steady process, but remembering the geological setting there might be another explanation: as the slopes evolved on periglacial drift cover - which is layered - each layer might cause one group. Group 1 is caused by the soil layer, group 2 by the upper layer draining at the interface of upper and intermediate layer (known SSF path), and group 3 drains between intermediate and basal layer. (or g1: upper-intermediate, g2: intermediate-basal, g3: basal-bedrock)

The fact that a bit of tracer recovery was measured at the source means that the level of the reservoir has to be temporally up to 2 m deep. The long recession curve of MQ could be linked to the slow drainage of the reservoir. The tracer was injected but did not have time to distribute in the reservoir. With decreasing water level it was stuck in the unsaturated zone. This would mean that tracer transport cannot be expected before the water level reaches injection depth (2 m).

If this concept can be assigned to the grassland and the coniferous hillslope in some way need further investigations. The role of bedrock remains unknown as the bedrock lies very deep and yet not much is known about its properties. It could not be measured with geoelectric and seismic methods (Wagner, 2014).

7 Conclusion

This study was designed and conducted to test different hypotheses on the origin of double-peak events. Although no significant conceptual errors occurred, it was not possible to test two of the stated hypotheses. In the study period very few precipitation events occurred, only two were sampled with high resolution and only one double-peak event occurred at all. Additionally, a particulary hot and dry summer restricted the reaction of discharge to precipitation events, as the water trickled into the dry ground or evaporated. The consequence of this was that almost no subsurface flow could be monitored. This leaves hypothesis one and two unsolved. To remember hypothesis one stated the origin of the double-peaks by HOF/SOF and flat SSF and hypothesis two by flat SSF and deep SSF. Only the third hypothesis could be investigated in more detail and the results in this study suggest that the geological boundary at site M has no effect on double-peak events. Here, it should be pointed out that just one double-peak event occurred during the study time and that differences exist between both discharge measurement sites along the creek.

Because of the dry and hot summer, other processes linked to runoff generation could be observed. The continuous drainage of the aquifer feeding the hillslope source - not interrupted by the input of new water - gave a good insight into the way the aquifer is structured and to the processes while draining. At the end of the summer, when discharge at the source was higher than at the catchment outlet, data were collected under extreme dry conditions. These might be quite unique data as such weather conditions did not occurred in the past years.

To complete the work done so far further investigations are necessary. To get at least some tracer response it is necessary to keep the monitoring network running. Of course, it will be difficult to get quantitative information due to sorption and degradation effects but hopefully qualitative information can be gained. And, in case of no tracer detection despite occurring SSF, hypothesis four could become more focussed: Maybe a yet unknown factor drives the double-peak events. Results in this study suggest that tracer injection in autumn/winter, and sampling of isotopes and hydrochemistry in the same period, would be useful to complete the current investigations - provided that this is not impaired by winter freeze. Another tracer experiment could also be conducted during summer - with more rainfall.

Bibliography

Anderson, a. E., Weiler, M., Alila, Y., and Hudson, R. O. (2009). Dye staining and excavation of a lateral preferential flow network. *Hydrology and Earth System Sciences*, 13(6):935–944.

Anderson, S. P., Dietrich, W. E., Montgomery, D. R., Torres, R., Conrad, M. E., and Loague, K. (1997). Subsurface flow paths in a steep, unchanneled catchment. *Water Resources Research*, 33(12):2637–2653.

Bachmair, S. (2012). Experimental investigation of hillslope hydrological dynamics by.

Bachmair, S. and Weiler, M. (2011). Forest Hydrology and Biogeochemistry. 216:455–481.

Bachmair, S. and Weiler, M. (2012). Hillslope characteristics as controls of subsurface flow variability. *Hydrology and Earth System Sciences*, 16(10):3699–3715.

Bachmair, S. and Weiler, M. (2014). Interactions and connectivity between runoff generation processes of different spatial scales. *Hydrological Processes*, 28(4):1916–1930.

Bachmair, S., Weiler, M., and Troch, P. a. (2012). Intercomparing hillslope hydrological dynamics: Spatio-temporal variability and vegetation cover effects. *Water Resources Research*, 48(5):n/a–n/a.

Blume, T., Zehe, E., Reusser, D. E., Iroumé, A., and Bronstert, A. (2008). Investigation of runoff generation in a pristine, poorly gauged catchment in the Chilean Andes I: A multi-method experimental study. *Hydrological Processes*, 22:3661–3675.

Bracken, L. J. and Croke, J. (2007). The concept of hydrological connectivity and its contribution to understanding runoff-dominated geomorphic systems. *Hydrological Processes*, 21(14 February 2007):1749–1763.

Buttle, J. M. (2002). Coupled vertical and lateral preferential flow on a forested slope. *Water Resources Research*, 38(5):10–1–10–9.

Corradini, C., Morbidelli, R., and Melone, F. (1998). On the interaction between infiltration and Hortonian runoff. *Journal of Hydrology*, 204(1-4):52–67.

Crockford, R. H. and Richardson, D. P. (2000). Partitioning of rainfall into throughfall, stemflow and interception: effect of forest type, ground cover and climate. *Hydrological processes*, 14(April 1999):2903–2920.

Doerr, S. H., Shakesby, R. a., and Walsh, R. P. D. (2000). Soil water repellency: Its causes, characteristics and hydro-geomorphological significance. *Earth Science Reviews*, 51(1-4):33–65.

Dunne, T. (1978). Field Studies of Hillslope Flow Processes.

Falasca, G. (2014). Untersuchung der lokalen Zuflüsse zum Bach in einem kleinen Einzugsgebiet im Gneis.

Flury, M. (2003). Dyes as tracers for vadose zone hydrology. *Reviews of Geophysics*, 41(1):1002.

Gabrielli, C., McDonnell, J., and Jarvis, W. (2012). The role of bedrock groundwater in rainfall–runoff response at hillslope and catchment scales. *Journal of Hydrology*, 450-451:117–133.

Gerke, K. M., Sidle, R. C., and Mallants, D. (2015). Preferential flow mechanisms identified from staining experiments in forested hillslopes. *Hydrological Processes*, 4578(May):n/a–n/a.

Graham, C. B. and McDonnell, J. J. (2010). Hillslope threshold response to rainfall: (2) Development and use of a macroscale model. *Journal of Hydrology*, 393(1-2):77–93.

Johnson, M. S. and Lehmann, J. (2006). Double-funneling of trees: Stemflow and root-induced preferential flow. *Ecoscience*, 13(3):324–333.

Jost, G., Heuvelink, G. B. M., and Papritz, a. (2005). Analysing the space-time distribution of soil water storage of a forest ecosystem using spatio-temporal kriging. *Geoderma*, 128(3-4 SPEC. ISS.):258–273.

Käss, W. (2004). *Lehrbuch der Hydrogeologie Band 9, Geohydrologische Markierungstechnik*. Gebrüder Borntraeger, berlin 199 edition.

Klaus, J. and Mcdonnell, J. J. (2013). Hydrograph separation using stable isotopes : Review and evaluation. *JOURNAL OF HYDROLOGY*, 505:47–64.

Lange, B., Luescher, P., and Germann, P. F. (2008). Significance of tree roots for preferential infiltration in stagnic soils. *Hydrology and Earth System Sciences Discussions*, 5:2373–2407.

Leibundgut, C., Maloszewski, P., and Külls, C. (2009). *Tracers in Hydrology*. John Wiley and Sons Ltd.

Levia, D. F., Van Stan, J. T., Mage, S. M., and Kelley-Hauske, P. W. (2010). Temporal variability of stemflow volume in a beech-yellow poplar forest in relation to tree species and size. *Journal of Hydrology*, 380(1-2):112–120.

McDonnell, J., Owens, I. F., and Stewart, M. (1991). A Case Study of Shallow Flow Paths in a Steep Zero-order Basin. *Water Resources Bulletin*, 27(4):679–685.

McGuire, K., Weiler, M., and McDonnell, J. (2007). Integrating tracer experiments with modeling to assess runoff processes and water transit times. *Advances in Water Resources*, 30(4):824–837.

McGuire, K. J. and McDonnell, J. J. (2010). Hydrological connectivity of hillslopes and streams: Characteristic time scales and nonlinearities. *Water Resources Research*, 46(10):n/a–n/a.

McNamara, J. P., Chandler, D., Seyfried, M., and Achet, S. (2005). Soil moisture states, lateral flow, and streamflow generation in a semi-arid, snowmelt-driven catchment. *Hydrological Processes*, 19(20):4023–4038.

Nordmann, B., Göttlein, A., and Binder, F. (2009). Influence of different tree species on runoff formation – an example of a catchment in the low-mountain range Franconian Forest, Germany. *Hydrologie und Wasserbewirschaftung*, 53(2):80–95.

Ritter, M. (2013). Combined field- and model-based intercomparison of hillslope hydrological dynamics Combined field- and model-based intercomparison of hillslope hydrological dynamics.

Sato, Y., Kumagai, T., Kume, A., Otsuki, K., and Ogawa, S. (2004). Experimental analysis of moisture dynamics of litter layers - The effects of rainfall conditions and leaf shapes. *Hydrological Processes*, 18(16):3007–3018.

Scherrer, S. and Naef, F. (2003). A decision scheme to indicate dominant hydrological flow processes on temperate grassland. *Hydrological Processes*, 17(2):391–401.

Scherrer, S., Naef, F., Faeh, a. O., and Cordery, I. (2006). Formation of runoff at the hillslope scale during intense precipitation. *Hydrology and Earth System Sciences Discussions*, 3:2523–2558.

Schmocker-Fackel, P. (2004). A Method to Delineate Runoff Processes in a Catchment and its Implications for Runoff Simulation. (15638):187.

Schume, H., Jost, G., and Hager, H. (2004). Soil water depletion and recharge patterns in mixed and pure forest stands of European beech and Norway spruce. *Journal of Hydrology*, 289(1-4):258–274.

Sidle, R. C., Hirano, T., Gomi, T., and Terajima, T. (2007). Hortonian overland flow from Japanese forest plantations—an aberration, the real thing, or something in between? *HYDROLOGICAL PROCESSES*, 21(November 2008):3237–3247.

Smart, P. and Smith, D. (1976). Water tracing in tropical regions, the use of fluorometric techniques in Jamaica. *Journal of Hydrology*, 30:179–195.

Spence, C. and Woo, M.-k. (2003). Hydrology of subarctic Canadian shield: soil-filled valleys. *Journal of Hydrology*, 279(1-4):151–166.

Troch, P. A., Paniconi, C., and Emiel van Loon, E. (2003). Hillslope-storage Boussinesq model for subsurface flow and variable source areas along complex hillslopes: 1. Formulation and characteristic response. *Water Resour. Res.*, 39(11):1316.

Tromp-Van Meerveld, H. J. and McDonnell, J. J. (2006a). Threshold relations in subsurface stormflow: 1. A 147-storm analysis of the Panola hillslope. *Water Resources Research*, 42(2):1–11.

Tromp-Van Meerveld, H. J. and McDonnell, J. J. (2006b). Threshold relations in subsurface stormflow: 2. The fill and spill hypothesis. *Water Resources Research*, 42(2):1–11.

Tromp-van Meerveld, H. J., Peters, N. E., and Mcdonnell, J. J. (2007). Effect of bedrock permeability on subsurface stormflow and the water balance of a trenched hillslope at the Panola Mountain Research Watershed , Georgia , USA. 769(September 2006):750–769.

Tromp-van Meerveld, I. and Weiler, M. (2008). Hillslope dynamics modeled with increasing complexity. *Journal of Hydrology*, 361(1-2):24–40.

Tsuboyama, Y., Sidle, R. C., Noguchi, S., and Hosoda, I. (1994). Flow and solute transport through the soil matrix and macropores of a hillslope segment. *Water Resources Research*, 30(4):879–890.

Uchida, T., Kosugi, K., and Mizuyama, T. (2001). Effects of pipeflow on hydrological process and its relation to landslide: A review of pipeflow studies in forested headwater catchments. *Hydrological Processes*, 15(July 2000):2151–2174.

Uchida, T., McDonnell, J. J., and Asano, Y. (2006). Functional intercomparison of hillslopes and small catchments by examining water source, flowpath and mean residence time. *Journal of Hydrology*, 327(3-4):627–642.

Uhlenbrook, S., Didszun, J., and Wenninger, J. (2008). Source areas and mixing of runoff components at the hillslope scale—a multi-technical approach. *Hydrological Sciences Journal*, 53(4):741–753.

Vogel, T., Sanda, M., Dusek, J., Dohnal, M., and Votrubova, J. (2010). Using Oxygen-18 to Study the Role of Preferential Flow in the Formation of Hillslope Runoff. *Vadose Zone Journal*, 9(2):252.

Völkel, J., Leopold, M., and Roberts, M. C. (2001). The radar signatures and age of periglacial slope deposits, Central Highlands of Germany. *Permafrost and Periglacial Processes*, 12(4):379–387.

Wagener, T., Sivapalan, M., Troch, P., and Woods, R. (2007). Catchment Classification and Hydrologic Similarity. *Geography Compass*, 1:1–31.

Wagner, M. (2014). Geoelektrische Untersuchung von Hängen zur Bestimmung der Verwitterungstiefe. (September).

Weiler, M. and McDonnell, J. (2004). Virtual experiments: A new approach for improving process conceptualization in hillslope hydrology. *Journal of Hydrology*, 285(1-4):3–18.

Weiler, M. and McDonnell, J. J. (2007). Conceptualizing lateral preferential flow and flow networks and simulating the effects on gauged and ungauged hillslopes. *Water Resources Research*, 43(3):1–13.

Weiler, M., McDonnell, J. J., Tromp-van Meerveld, I., and Uchida, T. (2006). Subsurface Stormflow. In *Encyclopedia of Hydrological Sciences*. John Wiley & Sons, Ltd.

Weiler, M. and Naef, F. (2003). An experimental tracer study of the role of macropores in infiltration in grassland soils. *Hydrological Processes*, 17(2):477–493.

Wernli, H. (2003). Einführung in die Tracerhydrologie. *Geographisches Institut der Universität Bern*.

Wienhöfer, J., Germer, K., Lindenmaier, F., Färber, A., and Zehe, E. (2009). Applied tracers for the observation of subsurface stormflow at the hillslope scale. *Hydrology and Earth System Sciences Discussions*, 6:2961–3006.